INTERNATIONAL JOURNAL OF
NUMERICAL ANALYSIS AND MODELING
Volume 19, Number 6, Pages 739–760

A DECOUPLED, PARALLEL, ITERATIVE FINITE ELEMENT METHOD FOR SOLVING THE STEADY BOUSSINESQ EQUATIONS

YUANYUAN HOU, WENJING YAN*, LIOBA BOVELETH, AND XIAOMING HE

Abstract. In this work, a decoupled, parallel, iterative finite element method for solving the steady Boussinesq equations is proposed and analyzed. Starting from an initial guess, an iterative algorithm is designed to decouple the Naiver-Stokes equations and the heat equation based on certain explicit treatment with the solution from the previous iteration step. At each step of the iteration, the two equations can be solved in parallel by using finite element discretization. The existence and uniqueness of the solution to each step of the algorithm is proved. The stability analysis and error estimation are also carried out. Numerical tests are presented to verify the analysis results and illustrate the applicability of the proposed method.

Key words. Steady Boussinesq equations, decoupled parallel iterative algorithm, finite element method, error analysis.

1. Introduction

The system of Boussinesq equations is an important model in fluid dynamics, describing incompressible flow driven by heat difference, namely the natural convection phenomenon. The typical examples of the convection can be found in nature, such as the ocean flow driven by temperature difference, the ventilation in a room, and the ground water system (see [20, 48, 50, 63, 75, 80]). In engineering, free convection is exploited in numerous applications, such as double-glazed windows, cooling in small electronic devices, building insulation, and environmental transport problems (see [4, 21, 37, 47, 49, 78]).

In the Boussinesq model, the density of the fluid is kept constant and the gravitational force depends on the temperature. In this approximation, the fluid and the temperature are coupled by two terms. The first one is a buoyancy term, which linearly depends on the temperature and acts in the direction opposite to the gravity, in the stationary incompressible Navier-Stokes equations of the fluid variables. The second one is a convective term, which is based on the velocity of the fluid, in the convection-diffusion equation of the temperature variable.

In this work, the stationary Boussinesq equations are considered:

$$(\mathbf{u}\cdot\nabla)\mathbf{u} - Pr\Delta\mathbf{u} + \nabla p = PrRa\hat{\mathbf{g}}\theta + \boldsymbol{\gamma}_1, \text{ in } \Omega, \tag{1}$$

$$\nabla\cdot\mathbf{u} = 0, \text{ in } \Omega, \tag{2}$$

$$\mathbf{u} = \mathbf{0}, \text{ on } \partial\Omega, \tag{3}$$

$$\mathbf{u}\cdot\nabla\theta - k_0\Delta\theta = \gamma_2, \text{ in } \Omega, \tag{4}$$

$$\theta = 0 \text{ on } \Gamma_0, \ \nabla\theta\cdot\mathbf{n} = 0 \text{ on } \partial\Omega\setminus\Gamma_0, \ |\Gamma_0| \neq 0. \tag{5}$$

Received by the editors November 27, 2021 and, in revised form February 18, 2022; accepted February 22, 2022.

2000 *Mathematics Subject Classification.* 35Q30, 65N12, 65N15, 65N30, 76D05, 76R10.

*Corresponding author.

Here Ω is a bounded domain in R^d with Lipschitz continuous boundary $\partial\Omega$, where $d = 2, 3$ is the space dimension. Γ_0 is part of $\partial\Omega$ with its measure $|\Gamma_0| \neq 0$. $\mathbf{u}$ is the fluid velocity, p the pressure, and θ the temperature. Furthermore, $\boldsymbol{\gamma}_1$ and γ_2 are the given force functions in $[H^{-1}(\Omega)]^d$ and $H^{-1}(\Omega)$, respectively. Pr and Ra are Prandtl and Rayleigh numbers, respectively. k_0 is the thermal conductivity parameter. $\hat{\mathbf{g}} = \mathbf{g}/|\mathbf{g}|$ is the unified gravitational acceleration. Throughout this paper, vector valued functions are denoted by boldface.

The stationary Boussinesq equations (1)-(5) include, in addition to the velocity and the pressure fields, the temperature field, making it non-trivial to find the numerical solution. Early attempts on finding efficient numerical schemes to solve (1)-(5) were coupled finite element methods, such as the standard Galerkin finite element method [5], the low-order nonconforming finite element method [72], the least squared finite element method [57], the projection-based stabilized mixed finite element method [14], and the two-level finite element method [41]. These methods usually lead to coupled large systems to solve for $\mathbf{u}$, p, and θ simultaneously. Furthermore, the systems are also nonlinear and need iterations to handle the nonlinearity.

Exploiting the existing computing resources, various decoupled methods can reduce the computational cost by solving several smaller problems, be easily implemented based on the legacy code of the smaller problems, and speed up the computation by parallel computation, such as the iterative domain decomposition methods [6, 7, 9, 10, 11, 12, 22, 23, 24, 25, 28, 29, 30, 39, 53, 54, 55, 66, 79, 84], non-iterative domain decomposition methods [13, 18, 19, 26, 27, 36, 40, 65, 73, 104, 105], two-grid methods [2, 8, 60, 61, 82, 83], partition time-stepping methods [17, 62, 68], Lagrange multiplier methods [3, 34, 51, 103], explicit-implicit linearized stablization schemes [31, 32, 45, 58, 59, 71, 87, 94, 95, 102], the Invariant Energy Quadratization (IEQ) method [15, 81, 88, 90, 91, 92, 97, 99], the Scalar Auxiliary Variable (SAV) method [33, 52, 64, 69, 70, 98, 100], the zero-energy-contribution technique [85, 86, 87, 89, 96], and others [38, 46, 56, 67].

To avoid resulting large coupled systems, decoupled methods were also developed for the Boussinesq equations. By utilizing the data generated from previous iterative steps or temporal steps, the decoupled methods can decompose the original problem into several subsystems with smaller scales, and usually turn the original nonlinear problem into linearized ones. For stationary Boussinesq equations, the sequential iterative methods [42, 43] and two grid methods [74] are developed to decouple this problem. For the time-dependent case, an implicit-explicit (IMEX) scheme is proposed to decouple the system and solve the decoupled equations sequentially [93]. Extrapolation of velocities in previous temporal steps provides a prediction in the convection-diffusion equation, which decouples the whole system and linearizes the trilinear term in the convection-diffusion equation. Then the Navier-Stokes part is solved by using the solution obtained from the convection-diffusion equation.

In this paper, we aim to develop and analyze an efficient parallel iterative decoupling method for the stationary Boussinesq equations. The key technique is to design an iteration, which provides a convergent prediction for the coupling terms hence decouples the convection-diffusion equation from the Navier-Stokes equations. The decoupled subsystems do not have to wait for each other at each step of the iteration, thus can be solved in parallel. For the proposed method, we carry out the well-posedness, stability, and convergence analysis. Compared with the analysis in [5], a different mapping is introduced to prove the existence of the standard finite element method. It turns out to be a strictly contracting mapping and guarantees the uniqueness if a restriction on the boundary data is imposed. The exponential convergence of the algorithm is proved theoretically and then verified by numerical experiment results with $Ra = 10^3$.

The remainder of this article is organized as follows. In Section 2, the functional setting for the problem and some properties are introduced. In Section 3, the decoupled parallel iterative finite element method is presented. Furthermore, the existence and uniqueness of the solution, the stability and the error estimates are obtained for the proposed scheme. In Section 4, three numerical tests are presented, including one experiment to verify the convergence behavior of the algorithm, a cavity square flow problem, and an isolated island problem.

2. Functional setting of the problem

In order to present the variational formulation of the problem, we refer to [1] for the Sobolev spaces $L^p(\Omega)$, $L^\infty(\Omega)$, $H^m(\Omega)$, and $H_0^m(\Omega)$ with the regular norms defined for them. Particularly, the following Hilbert spaces are introduced:

$$H_\Gamma^1(\Omega) = \left\{u \in H^1(\Omega)|\ u|_\Gamma = 0\},\ L_0^2(\Omega) = \{q \in L^2(\Omega)| \int_\Omega q \mathrm{d}\mathbf{x} = 0\right\}.$$

Note that the definitions here and hereafter include the case $\Gamma = \partial\Omega$, where $H_\Gamma^1(\Omega)$ degenerates to $H_0^1(\Omega)$. By virtue of Poincaré inequality, the H^1 semi-norm is a norm on $H_\Gamma^1(\Omega)$ if $|\Gamma| \neq 0$. Furthermore, the norm on $L_0^2(\Omega)$ is the usual $L^2(\Omega)$ norm. For convenience, $\|\cdot\|_{L^4(\Omega)}$, $\|\cdot\|_{L^2(\Omega)}$, $\|\cdot\|_{L^\infty(\Omega)}$, and $\|\cdot\|_{H^1(\Omega)}$ are denoted by $\|\cdot\|_{0,4}$, $\|\cdot\|_{0,2}$, $\|\cdot\|_{0,\infty}$, and $\|\cdot\|_1$, respectively and $|\cdot|_{H^m(\Omega)}$ is denoted by $|\cdot|_m$. For the d-dimensional case, the H^1 norm is defined as

$$|\mathbf{u}|_1 = \left(\sum_{i=1}^d |u_i|_1^2\right)^{1/2},\ \ \mathbf{u} \in [H_\Gamma^1(\Omega)]^d.$$

In addition, the H^m norm on multidimensional cases can be defined similarly.

We denote $l(\cdot) = \langle l, \cdot\rangle$, if l is a continuous linear functional on the spaces $[H_0^1(\Omega)]^d$ or $H_{\Gamma_0}^1(\Omega)$. For $H_{\Gamma_0}^1(\Omega)$, γ_2 belongs to $H^{-1}(\Omega)$ and the norm on it is defined as $\|\gamma_2\|_{-1} = \sup_{s\in H_{\Gamma_0}^1(\Omega)}\langle\gamma_2, s\rangle/\|s\|_1$. For $[H_0^1(\Omega)]^d$, $\boldsymbol{\gamma}_1 \in [H^{-1}(\Omega)]^d$ and its norm can be chosen as any kind of norm on the product space, such as $\|\boldsymbol{\gamma}\|_{[H^{-1}(\Omega)]^d} := \sum_{i=1}^d \|\gamma_i\|_{-1}$ for $\boldsymbol{\gamma} = (\gamma_i)_{i=1}^d$. For convenience, $\|\cdot\|_{[H^{-1}(\Omega)]^d}$ is denoted as $\|\cdot\|_{-1}$.

We set $V = \{\mathbf{u} \in [H_0^1(\Omega)]^d|\ \nabla\cdot\mathbf{u} = 0\}$. Moreover, to provide the definitions of the bilinear and trilinear functionals of the problem, we set $W = [H_0^1(\Omega)]^d$, $Q = L_0^2(\Omega)$, $S = H_{\Gamma_0}^1(\Omega)$, and define

$$\begin{aligned}
&a(\mathbf{u},\mathbf{v}) = \int_\Omega \nabla\mathbf{u} : \nabla\mathbf{v}\mathrm{d}\mathbf{x},\ \mathbf{u},\mathbf{v} \in W,\\
&\tilde{a}(\theta, s) = \int_\Omega \nabla\theta\cdot\nabla s\mathrm{d}\mathbf{x},\ \theta, s \in S,\\
&c(\mathbf{u},\mathbf{v},\mathbf{w}) = \frac{1}{2}\Big[\int_\Omega(\mathbf{u}\cdot\nabla)\mathbf{v}\cdot\mathbf{w}\mathrm{d}\mathbf{x} - \int_\Omega(\mathbf{u}\cdot\nabla)\mathbf{w}\cdot\mathbf{v}\mathrm{d}\mathbf{x}\Big],\ \mathbf{u}\in V,\ \mathbf{v},\mathbf{w}\in W,\\
&\tilde{c}(\mathbf{u},\theta,s) = \frac{1}{2}\Big[\int_\Omega(\mathbf{u}\cdot\nabla)\theta\cdot s\mathrm{d}\mathbf{x} - \int_\Omega(\mathbf{u}\cdot\nabla)s\cdot\theta\mathrm{d}\mathbf{x}\Big],\ \mathbf{u}\in V,\ \theta, s\in S,\\
&d(\mathbf{u}, q) = -\int_\Omega \nabla\cdot\mathbf{u}q\mathrm{d}\mathbf{x},\ \mathbf{u}\in W,\ q\in Q.
\end{aligned}$$

This leads to the following properties (see [5]).

Theorem 1. *There hold the estimates and identities below:*

$$|a(\mathbf{u},\mathbf{v})| \le |\mathbf{u}|_1|\mathbf{v}|_1,\ \mathbf{u},\mathbf{v}\in W, \tag{6}$$

$$a(\mathbf{u},\mathbf{u}) \ge |\mathbf{u}|_1^2,\ \mathbf{u}\in W, \tag{7}$$

$$|\tilde a(\theta,s)| \le |\theta|_1|s|_1,\ \theta,s\in S, \tag{8}$$

$$\tilde a(\theta,\theta) \ge |\theta|_1^2,\ \theta\in S, \tag{9}$$

$$|c(\mathbf{u},\mathbf{v},\mathbf{w})| \le \|\mathbf{u}\|_{0,4}|\mathbf{v}|_1\|\mathbf{w}\|_{0,4},\ \mathbf{u}\in V,\ \mathbf{v},\mathbf{w}\in W, \tag{10}$$

$$|c(\mathbf{u},\mathbf{v},\mathbf{w})| \le C_1|\mathbf{u}|_1|\mathbf{v}|_1|\mathbf{w}|_1,\ \mathbf{u},\mathbf{v},\mathbf{w}\in W, \tag{11}$$

$$c(\mathbf{u},\mathbf{v},\mathbf{w}) + c(\mathbf{u},\mathbf{w},\mathbf{v}) = 0,\ \mathbf{u}\in V,\ \mathbf{v},\mathbf{w}\in W, \tag{12}$$

$$|\tilde c(\mathbf{u},\theta,s)| \le \|\mathbf{u}\|_{0,4}|\theta|_1\|s\|_{0,4},\ \mathbf{u}\in V,\ \theta,s\in S, \tag{13}$$

$$|\tilde c(\mathbf{u},\theta,s)| \le C_2|\mathbf{u}|_1|\theta|_1|s|_1,\ \mathbf{u}\in W,\ \theta,s\in S, \tag{14}$$

$$\tilde c(\mathbf{u},\theta,s) + \tilde c(\mathbf{u},s,\theta) = 0,\ \mathbf{u}\in V,\ \theta,s\in S, \tag{15}$$

$$|(\mathbf{g}\hat{\theta},\mathbf{v})| \le C_3|\theta|_1|\mathbf{v}|_1,\ \theta\in S,\mathbf{v}\in W, \tag{16}$$

$$|\langle\boldsymbol{\gamma}_1,\mathbf{v}\rangle| \le \|\gamma_1\|_{-1}\|\mathbf{v}\|_1 \le C_4\|\gamma_1\|_{-1}|\mathbf{v}|_1,\ \mathbf{v}\in W, \tag{17}$$

$$|\langle\gamma_2,s\rangle| \le \|\gamma_2\|_{-1}\|s\|_1 \le C_5\|\gamma_2\|_{-1}|s|_1,\ s\in S. \tag{18}$$

The constants C_i, $i=1,\dots,5$ are positive real numbers depending on Ω.

Thus, the variational form of the problem is: Find $(\mathbf{u},p,\theta)\in W\times Q\times S$, such that

$$c(\mathbf{u},\mathbf{u},\mathbf{v}) + Pra(\mathbf{u},\mathbf{v}) + d(\mathbf{v},p) - PrRa(\hat{\mathbf{g}}\theta,\mathbf{v}) = \langle\boldsymbol{\gamma}_1,\mathbf{v}\rangle,\ \forall\mathbf{v}\in W, \tag{19}$$

$$d(\mathbf{u},q) = 0,\ \forall q\in Q, \tag{20}$$

$$\tilde c(\mathbf{u},\theta,s) + k_0\tilde a(\theta,s) = \langle\gamma_2,s\rangle,\ \forall s\in S. \tag{21}$$

The variational problem has an equivalent form as follows [77]: Find $(\mathbf{u},p)\in V\times S$, such that

$$c(\mathbf{u},\mathbf{u},\mathbf{v}) + Pra(\mathbf{u},\mathbf{v}) - PrRa(\hat{\mathbf{g}}\theta,s) = \langle\boldsymbol{\gamma}_1,\mathbf{v}\rangle,\ \forall\mathbf{v}\in V, \tag{22}$$

$$\tilde c(\mathbf{u},\theta,s) + k_0\tilde a(\theta,s) = \langle\gamma_2,s\rangle,\ \forall s\in S. \tag{23}$$

The existence and uniqueness of the solution to (19)-(21) can be referred to [5].

3. Finite element approximation

Let $\mathcal{T}_h$ be a regular triangulation of Ω, with $h=\max\{\mathrm{diam}K|\ K\in\mathcal{T}_h\}$ (see [16]). For a specific triangulation $\mathcal{T}_h$, $W_h\times Q_h\times S_h$ are proper subspaces of $[H_0^1\Omega]^d\times L_0^2(\Omega)\times H_{\Gamma_0}^1(\Omega)$. The pair $W_h\times Q_h$ is assumed to satisfy the inf-sup condition, that is, there exists a positive constant β, such that $\forall q_h\in Q_h$,

$$\sup_{\mathbf{v}_h\in W_h}\frac{d(\mathbf{v}_h,q_h)}{|\mathbf{v}_h|_1} \ge \beta\|q_h\|_0. \tag{24}$$

3.1. The traditional coupled finite element method. To lay a solid foundation for the decoupled finite element method, in this section we first revisit the traditional coupled finite element method: Find $(\mathbf{u}_h,p_h,\theta_h)\in W_h\times Q_h\times S_h$ satisfying

$$\begin{aligned} c(\mathbf{u}_h,\mathbf{u}_h,\mathbf{v}_h) + Pra(\mathbf{u}_h,\mathbf{v}_h) + d(\mathbf{v}_h,p_h) - PrRa(\hat{\mathbf{g}}\theta_h,\mathbf{v}_h) &= \langle\boldsymbol{\gamma}_1,\mathbf{v}_h\rangle,\\ &\forall\mathbf{v}_h\in W_h,\end{aligned} \tag{25}$$

$$d(\mathbf{u}_h,q_h) = 0,\forall q_h\in Q_h, \tag{26}$$

$$\tilde c(\mathbf{u}_h,\theta_h,s_h) + k_0\tilde a(\theta_h,s_h) = \langle\gamma_2,s_h\rangle,\forall s_h\in S_h. \tag{27}$$

Set $V_h = \{\mathbf{v}_h \in W_h | \ d(\mathbf{v}_h, q_h) = 0, \ \forall q_h \in Q_h\}$. Then an equivalent problem to (25)-(27) is: Find $(\mathbf{u}_h, \theta_h) \in V_h \times S_h$, such that

$$c(\mathbf{u}_h, \mathbf{u}_h, \mathbf{v}_h) + Pra(\mathbf{u}_h, \mathbf{v}_h) - PrRa(\hat{\mathbf{g}}\theta_h, \mathbf{v}_h) = \langle \boldsymbol{\gamma}_1, \mathbf{v}_h \rangle, \forall \mathbf{v}_h \in V_h, \tag{28}$$

$$\tilde{c}(\mathbf{u}_h, \theta_h, s_h) + k_0 \tilde{a}(\theta_h, s_h) = \langle \gamma_2, s_h \rangle, \forall s_h \in S_h. \tag{29}$$

In [5], the proof for the existence for the continuous problem is completed by introducing an operator and proving the existence of a fixed-point with Leray-Schauder's fixed-point theorem. The uniqueness is derived by reductio ad absurdum. The proof of well-posedness of the discrete problem is omitted due to its similarity to the continuous ones. In this paper, by introducing a different operator and employing Brouwer's fixed-point theorem, we carry out the proof for Theorem 2, which shows the existence for the discrete problem. Then the uniqueness is shown by adding a condition to ensure the operator to be a strictly contracting mapping in the proof of Theorem 3.

Theorem 2. *The problem (28) to (29) has at least one solution.*

Proof. Due to inequalities (8)-(15), $\tilde{c}(\mathbf{u}_h, \cdot, \cdot) + k_0 \tilde{a}(\cdot, \cdot)$ is an elliptic and continuous bilinear form on $S_h \times S_h$. Hence, there exists an operator $F_h : V_h \to S_h$ such that $\tilde{c}(\mathbf{u}_h, F_h(\mathbf{u}_h), s_h) + k_0 \tilde{a}(F_h(\mathbf{u}_h), s_h) = \langle \gamma_2, s_h \rangle$, $\forall s_h \in S_h$. By setting $s_h = F_h(\mathbf{u}_h)$ it is easy to prove

$$|F_h(\mathbf{u}_h)|_1 \le C_5 k_0^{-1} \|\gamma_2\|_{-1}. \tag{30}$$

Next, we define a mapping $G_h : V_h \to V_h$, such that

$$c(\mathbf{u}_h, G_h(\mathbf{u}_h), \mathbf{v}_h) + Pra(G_h(\mathbf{u}_h), \mathbf{v}_h) - PrRa(\hat{\mathbf{g}} F_h(\mathbf{u}_h), \mathbf{v}_h) = \langle \boldsymbol{\gamma}_1, \mathbf{v}_h \rangle, \ \forall \mathbf{v}_h \in V_h. \tag{31}$$

The bilinear form $c(\mathbf{u}_h, \cdot, \cdot) + a(\cdot, \cdot)$ is continuous and elliptic on $V_h \times V_h$, which ensures $G_h(\mathbf{u}_h)$ to be well defined. The proof will be completed if G_h has a fixed-point. Setting $\rho = C_4 Pr^{-1} \|\boldsymbol{\gamma}_1\|_{-1} + C_3 C_5 Ra k_0^{-1} \|\gamma_2\|_{-1}$, $\overline{B(0, \rho)} \subset V_h$ is a convex compact ball in a finite dimensional space V_h. By Brouwer's fixed-point theorem, we intend to prove G_h is a continuous mapping from $\overline{B(0, \rho)}$ to $\overline{B(0, \rho)}$.

To prove that $G_h(\mathbf{u}_h)$ is bounded, let $\mathbf{v}_h = G_h(\mathbf{u}_h)$ in (31). It follows from (7), (12), (16), and (17) that

$$\begin{aligned} Pr|G_h(\mathbf{u}_h)|_1^2 &\le Pra(G_h(\mathbf{u}_h), G_h(\mathbf{u}_h)) \\ &= \langle \boldsymbol{\gamma}_1, \mathbf{v}_h \rangle + PrRa(\hat{\mathbf{g}} F_h(\mathbf{u}_h), G_h(\mathbf{u}_h)) \\ &\le (C_4 \|\boldsymbol{\gamma}_1\|_{-1} + C_3 PrRa|F_h(\mathbf{u}_h)|_1)|G_h(\mathbf{u}_h)|_1. \end{aligned}$$

Combined with (30), we obtain

$$|G_h(\mathbf{u}_h)|_1 \le C_4 Pr^{-1} \|\boldsymbol{\gamma}_1\|_{-1} + C_3 C_5 Ra k_0^{-1} \|\gamma_2\|_{-1} := \rho, \tag{32}$$

which implies G_h maps $\overline{B(0, \rho)}$ to $\overline{B(0, \rho)}$.

Next, we prove that G_h is continuous. Replace $\mathbf{u}_h$ with $\mathbf{u}_{hi}, \ i = 1, 2$ in (31) and subtract between these two cases,

$$\begin{aligned} c(\mathbf{u}_{h1} - \mathbf{u}_{h2}, G_h(\mathbf{u}_{h1}), \mathbf{v}_h) + c(\mathbf{u}_{h,2}, G_h(\mathbf{u}_{h1}) - G_h(\mathbf{u}_{h2}), \mathbf{v}_h) \\ + Pra(G_h(\mathbf{u}_{h1}) - G_h(\mathbf{u}_{h2}), \mathbf{v}_h) - PrRa(\hat{\mathbf{g}}(F_h(\mathbf{u}_{h1}) - F_h(\mathbf{u}_{h2})), \mathbf{v}_h) = 0. \end{aligned}$$

Setting $\mathbf{v}_h = G_h(\mathbf{u}_{h1}) - G_h(\mathbf{u}_{h2})$ and applying (7), (11), (12), and (16), there holds

$$|G_h(\mathbf{u}_{h1}) - G_h(\mathbf{u}_{h2})|_1 \le Pr^{-1} C_1 |G_h(\mathbf{u}_{h1})|_1 |\mathbf{u}_{h1} - \mathbf{u}_{h2}|_1 + C_3 Ra |F_h(\mathbf{u}_{h1}) - F_h(\mathbf{u}_{h2})|_1. \tag{33}$$

Replace $\mathbf{u}_h$ with $\mathbf{u}_{hi}$ and θ_h with $F_h(\mathbf{u}_{hi})$, $i = 1, 2$ in (29) and subtract one from the other. It follows that

$$k_0\tilde{a}((F_h(\mathbf{u}_{h1}) - F_h(\mathbf{u}_{h2})), s_h) = -\,\tilde{c}(\mathbf{u}_{h1} - \mathbf{u}_{h2}, F_h(\mathbf{u}_{h1}), s_h) - \tilde{c}(\mathbf{u}_{h2}, F_h(\mathbf{u}_{h1}) - F_h(\mathbf{u}_{h2}), s_h), \forall s_h \in S_h.$$

Then replacing s_h with $F_h(\mathbf{u}_{h1}) - F_h(\mathbf{u}_{h2})$ and using (14), we obtain

$$\begin{aligned} |F_h(\mathbf{u}_{h1}) - F_h(\mathbf{u}_{h2})|_1 \leq& C_2 k_0^{-1}|\mathbf{u}_{h1} - \mathbf{u}_{h2}|_1 |F_h(\mathbf{u}_{h1})|_1 \\ \leq& C_2C_5k_0^{-2}\|\gamma_2\|_{-1}|\mathbf{u}_{h1} - \mathbf{u}_{h2}|_1. \end{aligned} \tag{34}$$

Combining (32), (33), and (34), we obtain

$$\begin{aligned} |G_h(\mathbf{u}_{h1}) - G_h(\mathbf{u}_{h2})|_1 \leq& Pr^{-1}\big(C_1C_4Pr^{-1}\|\boldsymbol{\gamma}_1\|_{-1} + C_3C_5k_0^{-1}Ra(C_1 \\ &+ C_2Prk_0^{-1})\|\gamma_2\|_{-1}\big)|\mathbf{u}_{h1} - \mathbf{u}_{h2}|. \end{aligned} \tag{35}$$

This implies that G_h is continuous and completes the proof. $\square$

Remark 1. *Suppose u_h is a fixed-point of operator G_h in (32). We obtain the prior estimate of $\mathbf{u}_h$,*

$$|\mathbf{u}_h|_1 \leq C_4Pr^{-1}\|\boldsymbol{\gamma}_1\|_{-1} + C_3C_5k_0^{-1}Ra\|\gamma_2\|_{-1}. \tag{36}$$

The uniqueness of the solution to problem (28)-(29) is guaranteed under the assumption that the extension of the boundary data is sufficiently small, which will be demonstrated by Theorem 3. Before stating this theorem, the following notations are introduced.

$$N_h := \sup\{c(\mathbf{u}_h, \mathbf{v}_h, \mathbf{w}_h)|\ |\mathbf{u}_h|_1 = |\mathbf{v}_h|_1 = |\mathbf{w}_h|_1 = 1,\ \mathbf{u}_h, \mathbf{v}_h, \mathbf{w}_h \in V_h\}, \tag{37}$$

$$L_h := \sup\{\tilde{c}(\mathbf{u}_h, \theta_h, s_h)|\ |\mathbf{u}_h|_1 = |\theta_h|_1 = |s_h|_1 = 1,\ \mathbf{u}_h \in V_h, \theta_h, s_h \in S_h\}. \tag{38}$$

Theorem 3. *Suppose there holds the condition*

$$C_4N_hPr^{-1}\|\boldsymbol{\gamma}_1\|_{-1} + C_3C_5k_0^{-1}Ra(N_h + L_hPrk_0^{-1})\|\gamma_2\|_{-1} < Pr, \tag{39}$$

then (28)-(29) has one unique solution.

Proof. As N_h and L_h are sharper bounds for $c(\cdot,\cdot,\cdot)$ and $\tilde{c}(\cdot,\cdot,\cdot)$, we replace the constants C_1 and C_2 with N_h and L_h, respectively in (35) and obtain

$$\begin{aligned} |G_h(\mathbf{u}_{h1}) - G_h(\mathbf{u}_{h2})|_1 \leq& Pr^{-1}\big(C_4N_hPr^{-1}\|\boldsymbol{\gamma}_1\|_{-1} + C_3C_5k_0^{-1}Ra(N_h \\ &+ L_hPrk_0^{-1})\|\gamma_2\|_{-1}\big)|\mathbf{u}_{h1} - \mathbf{u}_{h2}|_1 \\ :=& \sigma|\mathbf{u}_{h1} - \mathbf{u}_{h2}|_1. \end{aligned}$$

Note that $\sigma < 1$ if (39) holds, implying that the operator G_h is a strict contracting mapping from V_h to V_h. Thus the uniqueness of the fixed-point is guaranteed. $\square$

3.2. The parallel, iterative, decoupled finite element method. In this section, we propose our parallel, iterative, decoupled scheme of the Boussinesq equations: Find $(\mathbf{u}_h^k, p_h^k, \theta_h^k) \in W_h \times Q_h \times S_h$, such that

$$c(\mathbf{u}_h^k, \mathbf{u}_h^k, \mathbf{v}_h) + Pra(\mathbf{u}_h^k, \mathbf{v}_h) + d(\mathbf{v}_h, p_h^k) - PrRa(\hat{\mathbf{g}}\theta_h^{k-1}, \mathbf{v}_h) = \langle\boldsymbol{\gamma}_1, \mathbf{v}_h\rangle, \quad \forall \mathbf{v}_h \in W_h, \tag{40}$$

$$d(\mathbf{u}_h^k, q_h) = 0, \forall q_h \in Q_h, \tag{41}$$

$$\tilde{c}(\mathbf{u}_h^{k-1}, \theta_h^k, s_h) + k_0\tilde{a}(\theta_h^k, s_h) = \langle\gamma_2, s_h\rangle, \forall s_h \in S_h, \tag{42}$$

where $(\mathbf{u}_h^0, p_h^0, \theta_h^0)$ are appropriately chosen initial guesses.

By employing the Newton iteration, the scheme can be linearized leading to the following algorithm.

Algorithm 1 The algorithm for solving (40)-(42).

Given initial $(\mathbf{u}_h^0, \theta_h^0) \in W_h \times Q_h$;
$ERR_1 = 10^9$; $k = 1$;
while $ERR_1 > \epsilon_S$, **do**
Procedure 1: Given initial guess $\mathbf{u}_h^{k,0}$;
$ERR_2 = 10^9$; $l = 1$;
while $ERR_2 > \epsilon_N$, **do**
Find $(\mathbf{u}_h^{k,l}, p_h^{k,l}) \in W_h \times Q_h$, such that

$$\begin{aligned} &c(\mathbf{u}_h^{k,l-1}, \mathbf{u}_h^{k,l}, \mathbf{v}_h) + c(\mathbf{u}_h^{k,l}, \mathbf{u}_h^{k,l-1}, \mathbf{v}_h) + Pra(\mathbf{u}_h^{k,l}, \mathbf{v}_h) + d(\mathbf{v}_h, p_h^{k,l}) \\ &- PrRa(\hat{\mathbf{g}}\theta_h^{k-1}, \mathbf{v}_h) = \langle \boldsymbol{\gamma}_1, \mathbf{v}_h \rangle + c(\mathbf{u}_h^{k,l-1}, \mathbf{u}_h^{k,l-1}, \mathbf{v}_h), \forall \mathbf{v}_h \in W_h, \end{aligned} \tag{43}$$

$$d(\mathbf{u}_h^{k,l}, q_h) = 0, \forall q_h \in Q_h, \tag{44}$$

Compute $ERR_2 = \|(\mathbf{u}_h^{k,l}, p_h^{k,l}) - (\mathbf{u}_h^{k,l-1}, p_h^{k,l-1})\|_N$;
$l = l + 1$;
end while
Procedure 2: Find $\theta_h^k \in S_h$, such that

$$\tilde{c}(\mathbf{u}_h^{k-1}, \theta_h^k, s_h) + k_0 \tilde{a}(\theta_h^k, s_h) = \langle \gamma_2, s_h \rangle, \forall s_h \in S_h. \tag{45}$$

Compute $ERR_1 = \|(\mathbf{u}_h^k, p_h^k, \theta_h^k) - (\mathbf{u}_h^{k-1}, p_h^{k-1}, \theta_h^{k-1})\|_S$;
$k = k + 1$;
end while

Remark 2. *$\|\cdot\|_S$ and $\|\cdot\|_N$ can be any chosen norms on $W_h \times Q_h \times S_h$ and $W_h \times Q_h$. ϵ_S and ϵ_N are error tolerances with respect to the iteration.*

Remark 3. *Procedure 1 and Procedure 2 are independent and implemented in parallel.*

Now we consider the existence and uniqueness of (40)-(42). We first recall the following theorem from [35].

Theorem 4. *Consider the abstract problem: Find $\mathbf{u} \in V$, such that*

$$a_1(\mathbf{u}, \mathbf{u}, \mathbf{v}) = \langle l, \mathbf{v} \rangle, \ \forall \mathbf{v} \in V. \tag{46}$$

Suppose there hold the following conditions:

- *(i) The bilinear form $a_1(\mathbf{w}, \cdot, \cdot)$ is uniformly elliptic with respect to $\mathbf{w}$, i.e., there exists a positive constant α, such that $a_1(\mathbf{w}, \mathbf{v}, \mathbf{v}) \geq \alpha \|\mathbf{v}\|_V^2$, $\forall \mathbf{w}, \mathbf{v} \in V$.*
- *(ii) There exists a continuous and nondecreasing function $L : R^+ \to R^+$, such that $\forall \mu > 0$, $|a_1(\mathbf{w}_1, \mathbf{u}, \mathbf{v}) - a_1(\mathbf{w}_2, \mathbf{u}, \mathbf{v})| \leq L(\mu) \|\mathbf{w}_1 - \mathbf{w}_2\|_V \|\mathbf{u}\|_V \|\mathbf{v}\|_V$, $\forall \mathbf{u}, \mathbf{v} \in V$, $\mathbf{w}_1, \mathbf{w}_2 \in S_\mu = \{\mathbf{w} \in V | \|\mathbf{w}\|_V \leq \mu\}$.*
- *(iii) $(\|l\|_{V'}/\alpha^2) L(\|l\|_{V'}/\alpha) < 1$.*

Then (46) has a unique solution.

By employing this theorem, we prove the existence and uniqueness of (40)-(42) presented below.

Theorem 5. *If $C_4 \|\boldsymbol{\gamma}_1\|_{-1} + C_3 C_5 PrRak_0^{-1} \|\gamma_2\|_{-1} < Pr^2 N_h^{-1}$, the problem (40)-(42) is solvable and has one unique solution.*

Proof. Let $\mathbf{v}_h \in V_h$ in (40)-(41). Then

$$c(\mathbf{u}_h^k, \mathbf{u}_h^k, \mathbf{v}_h) + Pra(\mathbf{u}_h^k, \mathbf{v}_h) = PrRa(\hat{\mathbf{g}}\theta_h^{k-1}, \mathbf{v}_h) + \langle \boldsymbol{\gamma}_1, \mathbf{v}_h \rangle, \forall \mathbf{v}_h \in V_h. \tag{47}$$

Set $a_1(\mathbf{w},\mathbf{u},\mathbf{v}) = c(\mathbf{w},\mathbf{u},\mathbf{v})+Pra(\mathbf{u},\mathbf{v})$, $\langle l,\mathbf{v}\rangle = PrRa(\hat{\mathbf{g}}\theta_h^{k-1},\mathbf{v}_h)+\langle\boldsymbol{\gamma}_1,\mathbf{v}_h\rangle$. Then it suffices to prove (i)-(iii). Based on (7), (11), and (12), (i) and (ii) can be proved as follows:

$$\begin{aligned} a_1(\mathbf{w}_h,\mathbf{v}_h,\mathbf{v}_h) = c(\mathbf{w}_h,\mathbf{v}_h,\mathbf{v}_h) + Pra(\mathbf{v}_h,\mathbf{v}_h) \geq Pr|\mathbf{v}_h|_1^2, \forall\mathbf{v}_h\in V_h,\\ |a_1(\mathbf{w}_{h1},\mathbf{u}_h,\mathbf{v}_h) - a_1(\mathbf{w}_{h2},\mathbf{u}_h,\mathbf{v}_h)| =& |c(\mathbf{w}_{h1}-\mathbf{w}_{h2},\mathbf{u}_h,\mathbf{v}_h)|\\ \leq& N_h|\mathbf{w}_{h1}-\mathbf{w}_{h2}|_1|\mathbf{u}_h|_1|\mathbf{v}_h|_1. \end{aligned}$$

Moreover, it follows from (16), (17), and (30) that

$$\begin{aligned} \|l\|_{V_h'} =& \sup_{\mathbf{v}_h\in V_h} |\langle\boldsymbol{\gamma}_1,\mathbf{v}_h\rangle + PrRa(\hat{\mathbf{g}}\theta_h^{k-1},\mathbf{v}_h)|/|\mathbf{v}_h|_1\\ \leq& C_4\|\boldsymbol{\gamma}_1\|_{-1} + C_3PrRa|\theta_h^{k-1}|_1\\ \leq& C_4\|\boldsymbol{\gamma}_1\|_{-1} + C_3C_5PrRak_0^{-1}\|\gamma_2\|_{-1}, \end{aligned}$$

which implies l is continuous. Thus, if $C_4\|\boldsymbol{\gamma}_1\|_{-1}+C_3C_5PrRak_0^{-1}\|\gamma_2\|_{-1} < Pr^2N_h^{-1}$, condition (iii) is satisfied. Hence problem (47) has one unique solution.

Before discussing the uniqueness and existence of p_h, we rewrite problem (40)-(41) as follows: Find $(\mathbf{u}_h^k,p_h^k)\in W_h\times Q_h$, such that

$$A(\mathbf{u}_h^k)\mathbf{u}_h^k + B^\star p_h^k = l \text{ in } W_h', \tag{48}$$

$$B\mathbf{u}_h^k = 0 \text{ in } Q_h', \tag{49}$$

where $\langle A(\mathbf{u}_h)\mathbf{v}_h,\mathbf{w}_h\rangle = a_1(\mathbf{u}_h,\mathbf{v}_h,\mathbf{w}_h)$, $\langle B\mathbf{v}_h,q_h\rangle = d(\mathbf{v}_h,q_h)$, $\mathbf{u}_h,\mathbf{v}_h,\mathbf{w}_h\in W_h$, $q_h\in Q_h$ and $B^\star$ is the dual operator of B. Define $V_h^0 = \{f\in W_h'|\langle f,\mathbf{v}_h\rangle = 0,\forall\mathbf{v}_h\in V_h\}$. It is easy to verify that $l - A(\mathbf{u}_h^k)\mathbf{u}_h^k$ is an element in V_h^0. By virtue of (24), $B^\star$ is an isomorphism from Q_h to V_h^0, (see [35]).

Thus, there exists one $p_h^k\in Q_h$, such that $B^\star p_h^k = l - A(\mathbf{u}_h^k)\mathbf{u}_h^k$ in V_h'. This implies that there exists one unique $(\mathbf{u}_h^k,p_h^k)$ as the solution to (40)-(41).

As (42) is a linear system, it is sufficient to prove that (42) has a unique solution or, equivalently, to prove that $\tilde{c}(\mathbf{u}_h^{k-1},\theta_h^k,s_h) + k_0\tilde{a}(\theta_h^k,s_h) = 0$, $\forall s_h\in S_h$ only has zero as solution. Set $s_h = \theta_h^k$, by (9) and (15), we have $k_0|\theta_h^k|_1^2 \leq \tilde{c}(\mathbf{u}_h^{k-1},\theta_h^k,\theta_h^k) + k_0\tilde{a}(\theta_h^k,\theta_h^k) = 0$. Thus $\theta_h^k = \mathbf{0}$ and we prove the theorem. □

3.3. Stability of the decoupled finite element method. In this section we consider the stability of the numerical schemes including the decoupled parallel iterative scheme and the Newton iteration. First, we present an estimate of the decoupled parallel iterative scheme's solution, which indicates the scheme is stable. Next, Theorem 7 shows that the linearized procedure is stable under certain conditions.

Theorem 6. *The solution to (40)-(42) satisfies*

$$|\mathbf{u}_h^k|_1 \leq C_4Pr^{-1}\|\boldsymbol{\gamma}_1\|_{-1} + C_3C_5Rak_0^{-1}\|\gamma_2\|_{-1}, \tag{50}$$

$$|\theta_h^k|_1 \leq C_5k_0^{-1}\|\gamma_2\|_{-1}, \tag{51}$$

for any integer $k\geq 1$, if the initial data of θ_h^0 satisfies $|\theta_h^0|_1 \leq C_5k_0^{-1}\|\gamma_2\|_{-1}$.

Proof. Choosing $\mathbf{v}_h = \mathbf{u}_h^k$ in (40) and employing the skew symmetry, we obtain

$$Pra(\mathbf{u}_h^k,\mathbf{u}_h^k) - PrRa(\hat{\mathbf{g}}\theta_h^{k-1},\mathbf{u}_h^k) = \langle\boldsymbol{\gamma}_1,\mathbf{u}_h^k\rangle.$$

By the ellipticity of $a(\cdot,\cdot)$, we have

$$Pr|\mathbf{u}_h^k|_1 \leq C_3PrRa|\theta_h^{k-1}|_1 + C_4\|\boldsymbol{\gamma}_1\|_{-1}. \tag{52}$$

Next, we set $s_h = \theta_h^k$ in (42), which leads to

$$|\theta_h^k|_1 \le C_5 k_0^{-1} \|\gamma_2\|_{-1}. \tag{53}$$

Combine (52) with (53), we prove the theorem. □

Theorem 7. *Suppose the following conditions hold:* $|\mathbf{u}_h^{k,0}|_1 < 1/4PrN_h^{-1}$ *and* $C_4\|\boldsymbol{\gamma}_1\|_{-1} + C_3C_5PrRak_0^{-1}\|\gamma_2\|_{-1} < 1/8Pr^2N_h^{-1}$. *Then the solution to (43)-(44)* $(\mathbf{u}_h^{k,l}, p_h^{k,l}) \in W_h \times Q_h$ *satisfies*

$$|\mathbf{u}_h^{k,l}|_1 \le 1/4PrN_h^{-1}, \tag{54}$$

$$|p_h^{k,l}|_1 \le 9/16Pr^2(\beta N_h)^{-1}. \tag{55}$$

Proof. Setting $\mathbf{v}_h = \mathbf{u}_h^{k,l}$ in (43), we obtain

$$\begin{aligned} Pra(\mathbf{u}_h^{k,l}, \mathbf{u}_h^{k,l}) =& \langle \boldsymbol{\gamma}_1, \mathbf{u}_h^{k,l}\rangle + c(\mathbf{u}_h^{k,l-1}, \mathbf{u}_h^{k,l-1}, \mathbf{u}_h^{k,l}) - c(\mathbf{u}_h^{k,l}, \mathbf{u}_h^{k,l-1}, \mathbf{u}_h^{k,l}) \\ &+ PrRa(\hat{\mathbf{g}}\theta_h^{k-1}, \mathbf{u}_h^{k,l}). \end{aligned}$$

By (7), (11), (16), and (17), we have

$$(Pr - N_h|\mathbf{u}_h^{k,l-1}|_1)|\mathbf{u}_h^{k,l}|_1 \le C_4\|\boldsymbol{\gamma}_1\|_{-1} + N_h|\mathbf{u}_h^{k,l-1}|_1^2 + C_3PrRa|\theta_h^{k-1}|_1.$$

Next, we use induction to prove the conclusion. Suppose $|\mathbf{u}_h^{k,l-1}|_1 < 1/4PrN_h^{-1}$ holds. By Theorem 6 and $C_4\|\boldsymbol{\gamma}_1\|_{-1} + C_3C_5PrRak_0^{-1}\|\gamma_2\|_{-1} < 1/8Pr^2N_h^{-1}$, there holds

$$\begin{aligned} |\mathbf{u}_h^{k,l}|_1 \le& (Pr - N_h|\mathbf{u}_h^{k,l-1}|_1)^{-1}(C_4\|\boldsymbol{\gamma}_1\|_{-1} + N_h|\mathbf{u}_h^{k,l-1}|_1^2 + C_3PrRa|\theta_h^{k-1}|_1) \\ \le& 1/4PrN_h^{-1}. \end{aligned} \tag{56}$$

Moreover, by (43), (24), and (56) we have

$$\begin{aligned} \beta\|p_h^{k,l}\|_0 \le& C_4\|\boldsymbol{\gamma}_1\|_{-1} + N_h|\mathbf{u}_h^{k,l-1}|_1^2 + 2N_h|\mathbf{u}_h^{k,l-1}|_1|\mathbf{u}_h^{k,l}|_1 + Pr|\mathbf{u}_h^{k,l}|_1 \\ &+ C_3PrRa|\theta_h^{k-1}|_1 \\ \le& C_4\|\boldsymbol{\gamma}_1\|_{-1} + C_3C_5PrRak_0^{-1}\|\gamma_2\|_{-1} + 7/16Pr^2/N_h, \\ \le& 9/16Pr^2/N_h, \end{aligned}$$

which leads to conclusion (55). □

3.4. Error analysis of the decoupled finite element method. In this subsection we carry out the error analysis for the decoupled parallel iterative scheme and Newton method. The total error estimates will be presented in Theorem 11. Moreover, the following approximation hypothesis are required. These abstract approximation properties will be fulfilled by specifically constructed finite dimensional spaces on triangulations of domain Ω.

Hypothesis 1. *There is an operator* $r_h \in L([H^3(\Omega) \cap H_0^1\Omega]^d, W_h)$, *such that* $\exists$ *a positive* C *such that* $\|\mathbf{v} - r_h\mathbf{v}\|_m \le Ch^{3-m}|\mathbf{v}|_3$, $\forall \mathbf{v} \in [H^3(\Omega) \cap H_0^1\Omega]^d$, *where* $m = 0, 1$.

Hypothesis 2. *There is an operator* $\pi_h \in L(H^2(\Omega), Q_h)$, *such that* $\exists$ *a positive* C *such that* $\|q - \pi_h q\|_{0,2} \le Ch^2|q|_2$, $\forall q \in H^2(\Omega)$.

Hypothesis 3. *There is an operator* $I_h \in L(H^3(\Omega) \cap H_{\Gamma_0}^1(\Omega), S_h)$, *such that* $\exists$ *a positive* C *such that* $\|\theta - I_h\theta\|_m \le Ch^{3-m}|\theta|_3$, $\forall \theta \in H^3(\Omega) \cap H_{\Gamma_0}^1(\Omega)$, *where* $m = 0, 1$.

Then we present the convergence analysis for the decoupled scheme.

Theorem 8. *Suppose $(\mathbf{u}_h^k,\theta_h^k)$ is a solution to (40)-(42) and*

$$C_4Pr^{-1}N_h\|\boldsymbol{\gamma}_1\|_{-1}+C_3C_5k_0^{-1}Ra(k_0^{-1}PrL_h+N_h)\|\gamma_2\|_{-1}<Pr. \tag{57}$$

Let $(\mathbf{u}_h,\theta_h)$ be a solution to (25)-(27). Then the iterative method (40)-(42) converges and there hold the error estimates. When $k=2m$, $m=1,2,\cdots$,

$$|\mathbf{u}_h^k-\mathbf{u}_h|_1\le\delta_1^m|\mathbf{u}_h^0-\mathbf{u}_h|_1, \tag{58}$$

$$|\theta_h^k-\theta_h|_1\le C_5k_0^{-2}L_h\|\gamma_2\|_{-1}\delta_0\delta_1^{m-1}|\theta_h^0-\theta_h|_1. \tag{59}$$

When $k=2m+1$, $m=0,1,2,\cdots$,

$$|\mathbf{u}_h^k-\mathbf{u}_h|_1\le\delta_0\delta_1^m|\theta_h^0-\theta_h|_1, \tag{60}$$

$$|\theta_h^k-\theta_h|_1\le C_5k_0^{-2}L_h\|\gamma_2\|_{-1}\delta_1^m|\mathbf{u}_h^0-\mathbf{u}_h|_1. \tag{61}$$

Here $\delta_1=C_5k_0^{-2}L_h\|\gamma_2\|_{-1}\delta_0$, $\delta_0=\big(Pr-N_h(C_3C_5k_0^{-1}Ra\|\gamma_2\|_{-1}+C_4Pr^{-1}\|\boldsymbol{\gamma}_1\|_{-1})\big)^{-1}\times C_3PrRa$.

Proof. It is easy to see that $(\mathbf{u}_h^k,\theta_h^k)$ is a solution to

$$c(\mathbf{u}_h^k,\mathbf{u}_h^k,\mathbf{v}_h)+Pra(\mathbf{u}_h^k,\mathbf{v}_h)-PrRa(\hat{\mathbf{g}}\theta_h^{k-1},\mathbf{v}_h)=\langle\boldsymbol{\gamma}_1,\mathbf{v}_h\rangle,\forall\mathbf{v}_h\in V_h, \tag{62}$$

$$\tilde{c}(\mathbf{u}_h^{k-1},\theta_h^k,s_h)+k_0\tilde{a}(\theta_h^k,s_h)=\langle\gamma_2,s_h\rangle,\forall s_h\in S_h. \tag{63}$$

Subtracting (62) from (28) yields

$$\begin{aligned}&c(\mathbf{u}_h^k,\mathbf{u}_h^k-\mathbf{u}_h,\mathbf{v}_h)+c(\mathbf{u}_h^k-\mathbf{u}_h,\mathbf{u}_h,\mathbf{v}_h)+Pra(\mathbf{u}_h^k-\mathbf{u}_h,\mathbf{v}_h)\\&-PrRa(\hat{\mathbf{g}}(\theta_h^{k-1}-\theta_h),\mathbf{v}_h)=0,\ \forall\mathbf{v}_h\in V_h.\end{aligned}$$

Set $\mathbf{v}_h=\mathbf{u}_h^k-\mathbf{u}_h$ and apply (7), (11), (12), and (16). Then we obtain

$$\begin{aligned}Pr|\mathbf{u}_h^k-\mathbf{u}_h|_1^2\le&-c(\mathbf{u}_h^k-\mathbf{u}_h,\mathbf{u}_h,\mathbf{u}_h^k-\mathbf{u}_h)+PrRa(\hat{\mathbf{g}}(\theta_h^{k-1}-\theta_h),\mathbf{u}_h^k-\mathbf{u}_h)\\\le&N_h|\mathbf{u}_h^k-\mathbf{u}_h|_1^2|\mathbf{u}_h|_1+C_3PrRa|\theta_h^{k-1}-\theta_h|_1|\mathbf{u}_h^k-\mathbf{u}_h|_1.\end{aligned}$$

By virtue of (36), we obtain

$$\begin{aligned}|\mathbf{u}_h^k-\mathbf{u}_h|_1\le&C_3PrRa(Pr-N_h|\mathbf{u}_h|_1)^{-1}|\theta_h^{k-1}-\theta_h|_1\\\le&\delta_0|\theta_h^{k-1}-\theta_h|_1,\end{aligned} \tag{64}$$

where $\delta_0=C_3PrRa\big(Pr-N_h(C_3C_5k_0^{-1}Ra\|\gamma_2\|_{-1}+C_4Pr^{-1}\|\boldsymbol{\gamma}_1\|_{-1})\big)^{-1}$. Subtracting (63) from (29), there holds

$$\tilde{c}(\mathbf{u}_h^{k-1}-\mathbf{u}_h,\theta_h^k,s_h)+\tilde{c}(\mathbf{u}_h,\theta_h^k-\theta_h,s_h)+k_0\tilde{a}(\theta_h^k-\theta_h,s_h)=0,\ \forall s_h\in S_h.$$

Let $s_h=\theta_h^k-\theta_h$ and employ (51). We obtain

$$|\theta_h^k-\theta_h|_1\le C_5k_0^{-2}L_h\|\gamma_2\|_{-1}|\mathbf{u}_h^{k-1}-\mathbf{u}_h|_1. \tag{65}$$

Combining (64) with (65),

$$\begin{aligned}|\mathbf{u}_h^k-\mathbf{u}_h|_1\le&\delta_0C_5L_hk_0^{-2}\|\gamma_2\|_{-1}|\mathbf{u}_h^{k-2}-\mathbf{u}_h|_1\\:=&\delta_1|\mathbf{u}_h^{k-2}-\mathbf{u}_h|_1.\end{aligned}$$

By employing induction, we obtain (58) and (60) and can verify $|\delta_1|<1$, which implies the procedure is convergent. (59) and (61) can be derived likewise by (65), (58), and (60). ∎

Next, we consider the convergence of the Newton iteration. Set the initial value $(\mathbf{u}_h^{k,0}, p_h^{k,0}) \in W_h \times Q_h$, such that

$$Pra(\mathbf{u}_h^{k,0}, \mathbf{v}_h) + d(\mathbf{v}_h, p_h^{k,0}) - PrRa(\hat{\mathbf{g}}\theta_h^{k-1}, \mathbf{v}_h) = \langle \boldsymbol{\gamma}_1, \mathbf{v}_h \rangle, \ \forall \mathbf{v}_h \in W_h, \tag{66}$$

$$d(\mathbf{u}_h^{k,0}, q_h) = 0, \ \forall q_h \in Q_h. \tag{67}$$

Then we come to the conclusion that:

Theorem 9. *Let* $\delta_3 = 2/\sqrt{3} N_h Pr^{-1}(C_4 Pr^{-1}\|\boldsymbol{\gamma}_1\|_{-1} + C_3 C_5 Ra k_0^{-1}\|\gamma_2\|_{-1})$ *and suppose* $|\delta_3| < 1$ *holds. Then, the Newton method converges and*

$$|\mathbf{u}_h^{k,l} - \mathbf{u}_h^k|_1 \leq 3/4 Pr N_h^{-1} \delta_3^{2^{l+1}}, \tag{68}$$

$$\|p_h^{k,l} - p_h^k\|_{0,2} \leq 27/16 Pr^2 (\beta N_h)^{-1} \delta_3^{2^{l+1}}. \tag{69}$$

Proof. The solution to (43)-(45) satisfies

$$\begin{aligned} &c(\mathbf{u}_h^{k,l-1}, \mathbf{u}_h^{k,l}, \mathbf{v}_h) + c(\mathbf{u}_h^{k,l}, \mathbf{u}_h^{k,l-1}, \mathbf{v}_h) + Pra(\mathbf{u}_h^{k,l}, \mathbf{v}_h) - PrRa(\hat{\mathbf{g}}\theta_h^{k-1}, \mathbf{v}_h) \\ &= \langle \boldsymbol{\gamma}_1, \mathbf{v}_h \rangle + c(\mathbf{u}_h^{k,l-1}, \mathbf{u}_h^{k,l-1}, \mathbf{v}_h), \forall \mathbf{v}_h \in V_h. \end{aligned} \tag{70}$$

Subtracting (70) from (62), we obtain

$$\begin{aligned} Pra(\mathbf{u}_h^{k,l} - \mathbf{u}_h^k, \mathbf{v}_h) =& c(\mathbf{u}_h^k - \mathbf{u}_h^{k,l-1}, \mathbf{u}_h^k - \mathbf{u}_h^{k,l-1}, \mathbf{v}_h) + c(\mathbf{u}_h^k - \mathbf{u}_h^{k,l}, \mathbf{u}_h^{k,l-1}, \mathbf{v}_h) \\ &+ c(\mathbf{u}_h^{k,l-1}, \mathbf{u}_h^k - \mathbf{u}_h^{k,l}, \mathbf{v}_h). \end{aligned}$$

Choose $\mathbf{v}_h = \mathbf{u}_h^{k,l} - \mathbf{u}_h^k$ and apply the ellipticity to get

$$\begin{aligned} Pr|\mathbf{u}_h^{k,l} - \mathbf{u}_h^k|_1^2 \leq& c(\mathbf{u}_h^k - \mathbf{u}_h^{k,l-1}, \mathbf{u}_h^k - \mathbf{u}_h^{k,l-1}, \mathbf{u}_h^{k,l} - \mathbf{u}_h^k) + c(\mathbf{u}_h^k - \mathbf{u}_h^{k,l}, \mathbf{u}_h^{k,l-1}, \\ & \mathbf{u}_h^{k,l} - \mathbf{u}_h^k) + c(\mathbf{u}_h^{k,l-1}, \mathbf{u}_h^k - \mathbf{u}_h^{k,l}, \mathbf{u}_h^{k,l} - \mathbf{u}_h^k) \\ \leq& N_h |\mathbf{u}_h^k - \mathbf{u}_h^{k,l-1}|_1^2 |\mathbf{u}_h^{k,l} - \mathbf{u}_h^k|_1 + N_h |\mathbf{u}_h^k - \mathbf{u}_h^{k,l}|_1^2 |\mathbf{u}_h^{k,l-1}|_1. \end{aligned}$$

Considering (54), there holds

$$|\mathbf{u}_h^{k,l} - \mathbf{u}_h^k|_1 \leq 4/3 Pr^{-1} N_h |\mathbf{u}_h^{k,l-1} - \mathbf{u}_h^k|_1^2 := \delta_2 |\mathbf{u}_h^{k,l-1} - \mathbf{u}_h^k|_1^2.$$

Next we will use induction to prove the result. Suppose (68) holds for $l-1$. For l we have

$$\begin{aligned} |\mathbf{u}_h^{k,l} - \mathbf{u}_h^k|_1 \leq& \delta_2 |\mathbf{u}_h^{k,l-1} - \mathbf{u}_h^k|_1^2 \\ \leq& \delta_2^{2^l - 1} |\mathbf{u}_h^{k,0} - \mathbf{u}_h^k|_1^{2^l}. \end{aligned}$$

Letting $\mathbf{v}_h \in V_h$ in (66), the initial value $\mathbf{u}_h^{k,0}$ satisfies

$$Pra(\mathbf{u}_h^{k,0}, \mathbf{v}_h) + d(\mathbf{v}_h, p_h^{k,0}) - PrRa(\hat{\mathbf{g}}\theta_h^{k-1}, \mathbf{v}_h) = \langle \boldsymbol{\gamma}_1, \mathbf{v}_h \rangle, \ \forall \mathbf{v} \in V_h.$$

Subtracting the identity from (47) and employing the inequalities in Theorem 1 along with (50), there holds the estimate of $|\mathbf{u}_h^{k,0} - \mathbf{u}_h^k|_1$,

$$|\mathbf{u}_h^{k,0} - \mathbf{u}_h^k|_1 \leq Pr^{-1} N_h (C_4 Pr^{-1}\|\boldsymbol{\gamma}_1\|_{-1} + C_3 C_5 Ra k_0^{-1}\|\gamma_2\|_{-1})^2.$$

Hence, we obtain (68).

Next we subtract (43) from (40) and obtain

$$\begin{aligned} d(\mathbf{v}_h, p_h^{k,l} - p_h^k) =& - Pra(\mathbf{u}_h^{k,l} - \mathbf{u}_h^k, \mathbf{v}_h) - c(\mathbf{u}_h^{k,l-1}, \mathbf{u}_h^{k,l} - \mathbf{u}_h^k, \mathbf{v}_h) \\ & - c(\mathbf{u}_h^{k,l} - \mathbf{u}_h^k, \mathbf{u}_h^{k,l-1}, \mathbf{v}_h) \\ & + c(\mathbf{u}_h^{k,l-1} - \mathbf{u}_h^k, \mathbf{u}_h^{k,l-1} - \mathbf{u}_h^k, \mathbf{v}_h), \ \forall \mathbf{v}_h \in W_h. \end{aligned}$$

By (24), (6), (11), (54), and (68), there holds

$$\begin{aligned}\beta\|p_h^{k,l}-p_h^k\|_{0,2} \leq&(Pr+2N_h|\mathbf{u}_h^{k,l-1}|_1)|\mathbf{u}_h^{k,l}-\mathbf{u}_h^k|_1+N_h|\mathbf{u}_h^{k,l-1}-\mathbf{u}_h^k|_1^2\\ \leq&9/8Pr^2N_h^{-1}\delta_3^{2^{l+1}}+9/16Pr^2N_h^{-1}\delta_3^{2^{l+1}}\\ \leq&27/16Pr^2N_h^{-1}\delta_3^{2^{l+1}},\end{aligned}$$

which leads to (69).

□

The total error estimates, which include the errors arising from the finite element method, the decoupled parallel iterative scheme, and the Newton iteration, are presented in Theorem 11. First we recall the following theorem regarding the errors of the coupled finite element method from [5].

Theorem 10. *Suppose the original problem (22)-(23) has a unique solution* $(\mathbf{u},\theta)$ *and* $(\mathbf{u}_h,\theta_h)$ *is the solution to (28)-(29). Then, there are positive constants* C_6-C_{10} *independent of* h*, such that*

$$|\mathbf{u}_h-\mathbf{u}|_1\leq C_6\inf_{q_h\in Q_h}\|p-q_h\|_{0,2}+C_7\inf_{\mathbf{v}_h\in W_h}|\mathbf{u}-\mathbf{v}_h|_1+C_8\inf_{s_h\in S_h}|\theta-s_h|_1, \tag{71}$$

$$|\theta_h-\theta|_1\leq C_9\inf_{s_h\in S_h}|\theta-s_h|_1+C_{10}|\mathbf{u}-\mathbf{u}_h|_1. \tag{72}$$

If the finite dimensional spaces are chosen to satisfy Hypothesis 1-3 (for example, Taylor-Hood element ([76]) for *u*-*p* and quadratic element for θ), then, based on the approximating property (see [16]), we obtain the total error estimates immediately.

Theorem 11. *Suppose the solution to (22)-(23) satisfies* $\mathbf{u}\in[H^3(\Omega)]^d\cap[H_0^1\Omega]^d$, $\theta\in H^3(\Omega)\cap H^1_{\Gamma_2}(\Omega)$, $p\in H^2(\Omega)\cap L_0^2(\Omega)$. $(\mathbf{u}_h^{k,l},\theta_h^k)$ *is a solution to (43)-(45). Then there holds: When* $k=2m$, $m=1,2,\cdots$,

$$\begin{aligned}|\mathbf{u}_h^{k,l}-\mathbf{u}|_1\leq&3/4PrN_h^{-1}\delta_3^{2^{l+1}}+\delta_1^m|\mathbf{u}_h^0-\mathbf{u}_h|_1+Ch^2|\mathbf{u}|_3+Ch^2|p|_2\\ &+Ch^2|\theta|_3,\end{aligned} \tag{73}$$

$$|\theta_h^k-\theta|_1\leq C_5k_0^{-2}L_h\|\gamma_2\|_{-1}\delta_0\delta_1^{m-1}|\theta_h^0-\theta_h|_1+Ch^2|\theta|_3+Ch^2|\mathbf{u}|_3. \tag{74}$$

When $k=2m+1$, $m=0,1,2,\cdots$,

$$\begin{aligned}|\mathbf{u}_h^{k,l}-\mathbf{u}|_1\leq&3/4PrN_h^{-1}\delta_3^{2^{l+1}}+\delta_0\delta_1^m|\theta_h^0-\theta_h|_1+Ch^2|\mathbf{u}|_3+Ch^2|p|_2\\ &+Ch^2|\theta|_3,\end{aligned} \tag{75}$$

$$|\theta_h^k-\theta|_1\leq C_5k_0^{-2}L_h\|\gamma_2\|_{-1}\delta_1^m|\mathbf{u}_h^0-\mathbf{u}_h|_1+Ch^2|\theta|_3+Ch^2|\mathbf{u}|_3. \tag{76}$$

Here δ_0, δ_1, δ_3, $\mathbf{u}_h^0$, θ_h^0 *are defined in Theorem 8 and 9 and* C *is independent of* h.

Proof. We prove the error estimate for $\mathbf{u}$ under the case $k=2m$, $m=1,2,\cdots$. By triangle inequality, there holds,

$$\begin{aligned}|\mathbf{u}_h^{k,l}-\mathbf{u}|_1\leq&|\mathbf{u}_h^{k,l}-\mathbf{u}_h^k|_1+|\mathbf{u}_h^k-\mathbf{u}_h|_1+|\mathbf{u}_h-\mathbf{u}|_1,\\ \leq&|\mathbf{u}_h^{k,l}-\mathbf{u}_h^k|_1+|\mathbf{u}_h^k-\mathbf{u}_h|_1+C_6\|p-\pi_hp\|_{0,2}+C_7|\mathbf{u}-r_h\mathbf{u}|_1\\ &+C_8|\theta-I_h\theta|_1.\end{aligned}$$

Employing (68), (58), and (71) along with Hypothesis 1-3, (73) holds. The rest of the proof can be completed likewise. □

Remark 4. *Concerning all the conditions related to Pr and Ra in Theorems 3, 5, 7, 8, and 9, the wellposedness and convergence of the scheme require that the following conditions hold:*

$$C_4\|\boldsymbol{\gamma}_1\|_{-1} + C_3C_5PrRa\frac{1}{k_0}\|\gamma_2\|_{-1} < \frac{1}{8}\frac{Pr^2}{N_h},$$
$$C_4\|\boldsymbol{\gamma}_1\|_{-1} + C_3C_5PrRa\frac{1}{k_0N_h}\left(\frac{1}{k_0}PrL_h + N_h\right)\|\gamma_2\|_{-1} < \frac{Pr^2}{N_h},$$

implying that

$$Pr > \max\left\{\sqrt{8C_4N_h\|\boldsymbol{\gamma}_1\|_{-1}}, 8C_3C_5N_hRa\frac{1}{k_0}\|\gamma_2\|_{-1}\right\},$$
$$Ra < \min\left\{\frac{k_0^2}{C_3C_5L_h}, \frac{k_0Pr}{8C_3C_5N_h\|\gamma_2\|_{-1}}\right\}.$$

4. Numerical examples

In this section, we present three numerical experiments to verify the theoretical analysis and illustrate the proposed method. In the first example, a problem with given accurate solution on $(0,1)\times(-0.25,0)$ is computed. As the solution is smooth enough, the convergence order of the scheme is dominated by properties of the finite element spaces, which is constructed by the Taylor-Hood elements and quadratic elements. We present the convergence orders and verify the conclusions under $Ra = 10^3$. In the second example, a cavity-flow problem is presented to further validate the proposed method. In the third example, an isolated island problem is simulated to test the behavior of the flow on less regular domains.

4.1. Example 1. The purpose of this example is to verify the numerical analysis in Section 3. Here, let the domain be $(0,1)\times(-0.25,0)$. The parameters of our problem are chosen as $Pr = 1$, $Ra = 10^3$, and $k_0 = 1$. The equations are solved on a uniform triangulation, in which the domain is divided into sub-rectangles by horizontal and vertical lines. A sub-rectangle is then divided into triangles by connecting the vertices from upper left to bottom right. The exact solution to this problem is chosen as follows:

$$\begin{aligned} u_1 &= x^2y^2 + \exp(-y), \\ u_2 &= -2/3xy^3 + 2 - \pi\sin(\pi x), \\ p &= -\big(2 - \pi\sin(\pi x)\big)\cos(2\pi y), \\ \theta &= \exp(x+y). \end{aligned}$$

Here, we consider the nonhomogeneous problem with the right-hand side of (1)-(5) set to fit the analytical solution. The iterative tolerances are set as $\epsilon_S = 10^{-9}$ and $\epsilon_N = 10^{-6}$ in (43)-(45). Then, we present the numerical results in Tables 1-3. Since the analytical solution is sufficiently smooth, the convergence orders are dominated by the orders of the polynomials. Hence, as shown in the tables, the convergence orders are optimal for the utilized Taylor-Hood elements and quadratic elements.

We also observe the convergence behavior of the iterative method on different meshes. Two cases with mesh edge size $h = 1/64$ and $h = 1/128$ are considered. As shown in Figures 1 and 2, the errors of $\mathbf{u}$, p, and θ reach the optimal convergence in Table 1 to Table 3 after the fifth iteration. In Figures 3 and 4, we obtain the solution to (40)-(42) at each iterative step and compute the errors between the solution of the decoupled finite element method and the solution of the standard

TABLE 1. The L^2 errors and corresponding convergence orders of decoupled parallel iterative finite element method for the steady Boussineq equations (1)-(5) with $Ra = 1000$.

$\frac{1}{h}$	L^2 Error **u**	Order	L^2 Error p	Order	L^2 Error θ	Order
4	2.7607e-03	-	8.2564e-02	-	6.9312e-05	-
8	3.564e-04	2.9534	2.2597e-02	1.8694	8.5992e-06	3.0108
16	4.4016e-05	3.0174	8.6689e-03	1.3822	1.0718e-06	3.0042
32	5.4798e-06	3.0058	2.4765e-03	1.8075	1.3389e-07	3.0009
64	6.8421e-07	3.0016	6.5585e-04	1.9169	1.6733e-08	3.0002
128	8.5497e-08	3.0005	1.6841e-04	1.9614	2.0916e-09	3.0001

TABLE 2. The H^1 errors and corresponding convergence orders of decoupled parallel iterative finite element method for the steady Boussinesq equations (1)-(5) with $Ra = 1000$.

$\frac{1}{h}$	H^1 Error **u**	Order	H^1 Error p	Order	H^1 Error θ	Order
4	80557e-02	-	2.3539e+00	-	2.6175e-03	-
8	2.0429e-02	1.9794	1.2647e+00	0.89627	6.5321e-04	2.0025
16	5.0681e-03	2.0111	6.3069e-01	1.0038	1.6323e-04	2.0006
32	1.2623e-03	2.0054	3.1369e-01	1.0076	4.0804e-05	2.0001
64	3.1523e-04	2.0016	1.5658e-01	1.0024	1.0201e-05	2
128	7.8782e-05	2.0004	7.8254e-02	1.0007	2.5502e-06	2

TABLE 3. The infinity errors and corresponding convergence orders of decoupled parallel iterative finite element method for the steady Boussinesq equations (1)-(5) with $Ra = 1000$.

$\frac{1}{h}$	Inf Error **u**	Order	Inf Error p	Order	Inf Error θ	Order
4	1.1759e-02	-	3.7727e-01	-	3.0632e-04	-
8	1.6853e-03	2.8027	1.3608e-01	1.4711	4.0349e-05	2.9244
16	2.0223e-04	3.0589	4.5862e-02	1.5691	5.181e-06	2.9612
32	2.5167e-05	3.0064	1.2533e-02	1.8716	6.5635e-07	2.9807
64	3.1048e-06	3.0189	3.251e-03	1.9468	8.2594e-08	2.9904
128	3.8464e-07	3.0129	8.2649e-04	1.9758	1.0359e-08	2.9952

coupled finite element method. In the standard finite element method, the Newton method is utilized with iterative tolerance set as $\epsilon = 10^{-9}$. We observe that the errors decrease fast. As for the errors of $\mathbf{u}$, the L^2 error descends all the way from 10^{-2} to 10^{-15} in twelve steps, which implies the exponential relation shown by the theoretical analysis in Theorem 8. A satisfying result can generally be achieved in five or six steps for all the variables. These indicate that the proposed method is efficient.

4.2. Example 2. In this subsection, a square cavity flow is presented to further illustrate the algorithm. The problem is considered on $\Omega = (0,1) \times (0,1)$. A Non-slip boundary condition is imposed for the velocity. The top horizontal wall of the square is adiabatic, i.e. $\frac{\partial \theta}{\partial \mathbf{n}} = 0$. Dirichlet conditions are imposed at the other walls, with $\theta = 0$ at the left and bottom wall, $\theta = 4y(1-y)$ at the right wall. The physical parameters are set as $Pr = 0.1$, $Ra = 10$, and $k_0 = 1$. The right hand

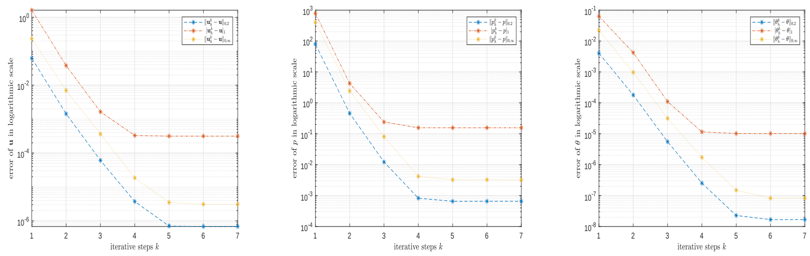

(A) Error of $\mathbf{u}$ (B) Error of p (C) Error of θ

FIGURE 1. The errors of the velocity $\mathbf{u}$, the pressure p, and the temperature θ in each iterative step k $(k = 1, 2, \dots, 5)$ of the decoupled parallel scheme with $Ra = 1000$ and mesh edge size $h = 1/64$.

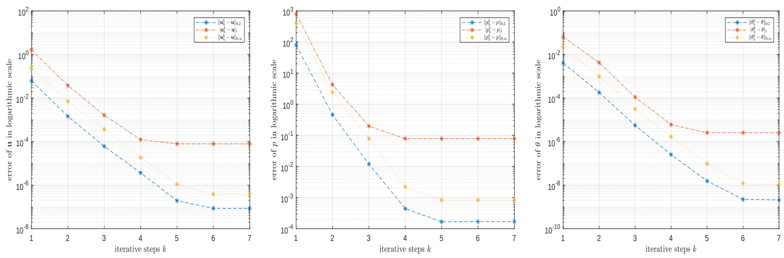

(A) Error of $\mathbf{u}$ (B) Error of p (C) Error of θ

FIGURE 2. The errors of the velocity $\mathbf{u}$, the pressure p and the temperature θ in each iterative step k $(k = 1, 2, \dots, 5)$ of the decoupled parallel scheme with $Ra = 1000$ and mesh edge size $h = 1/128$.

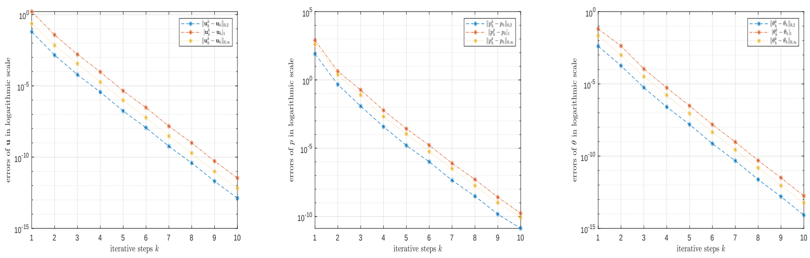

(A) Error of $\mathbf{u}$ (B) Error of p (C) Error of θ

FIGURE 3. The errors between solutions of (40)-(42) with solutions of standard finite element method at each iterative step k $(k = 1, 2, \dots, 10)$ with $Ra = 1000$ and mesh edge size $h = 1/64$.

side of the equation system is set as $\boldsymbol{\gamma}_1 = \mathbf{0}$ and $\gamma_2 = 0$. In contrast to the first experiment, we employ Delaunay triangulation to the square cavity. The boundary conditions are given in Figure 5. The resulting velocity fields and isotherms of the problem at mesh size $h = 0.02$ are shown in Figure 6, whose results are consistent with those in [101].

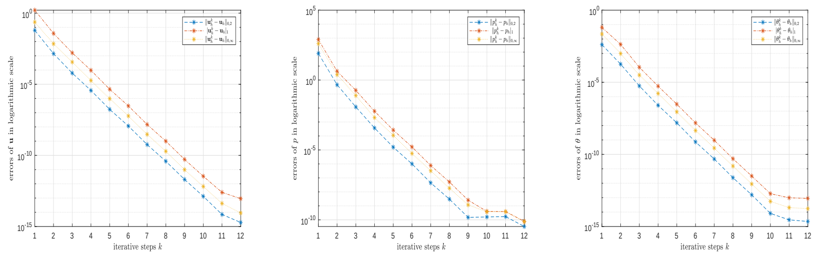

(A) Error of $\mathbf{u}$ (B) Error of p (C) Error of θ

FIGURE 4. The errors between solutions of (40)-(42) with solutions of standard finite element method at each iterative step k ($k = 1, 2, \ldots, 12$) with $Ra = 1000$ and mesh edge size $h = 1/128$.

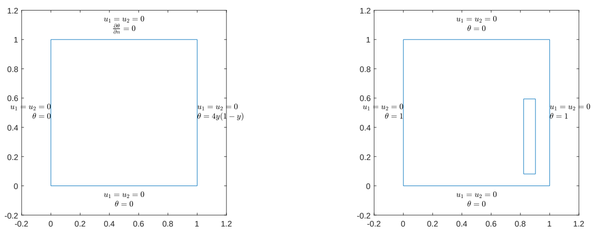

(A) The boundary conditions of Example 2 (B) The boundary conditions of Example 3

FIGURE 5. The geometry and the boundary conditions of the physical model.

4.3. Example 3. Finally, we simulate an isolated island problem [44]. The test is set up on a square cavity with an rectangular insulator, namely, $\Omega = (0,1) \times (0,1) \setminus (0.822, 0.903) \times (0.081, 0.594)$. We set $\frac{\partial \theta}{\partial \mathbf{n}} = 0$ on the boundary of the insulator. The geometry and other boundary conditions can be found in Figure 5. The physical parameters are $Pr = 0.01$, $Ra = 10^3$, $k_0 = 0.1$. The mesh is a Delaunay triangulation, again, with mesh size $h = 0.025$. The velocity field, isobar and isotherm are presented in Figure 7. The physically valid results further illustrate the applicability of the proposed method for a less regular domain.

5. Conclusions

In this work a decoupled, parallel, iterative scheme for the Boussinesq equations is proposed and analyzed. The existence and uniqueness of the scheme are proved. Numerical analysis shows that the scheme is stable and convergent with optimal convergence rates. A test exploiting the given analytical solution verifies the convergence behavior and shows that only five or six steps can already lead to a satisfying approximation of the solution of the problem. Two benchmarks are presented to show the applicability of the proposed method.

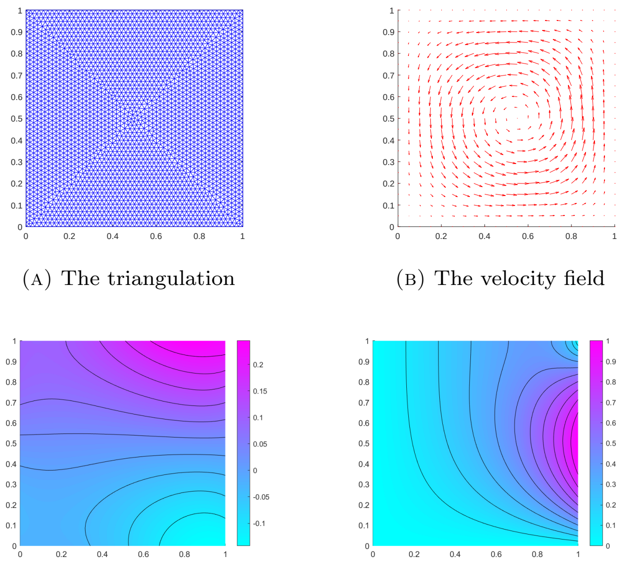

(A) The triangulation (B) The velocity field

(C) The isobar (D) The isotherm

FIGURE 6. The triangulation and the velocity field, isobar and isotherm of the cavity flow with $Pr = 0.1$, $Ra = 10$, $k_0 = 1$ at mesh size $h = 0.02$.

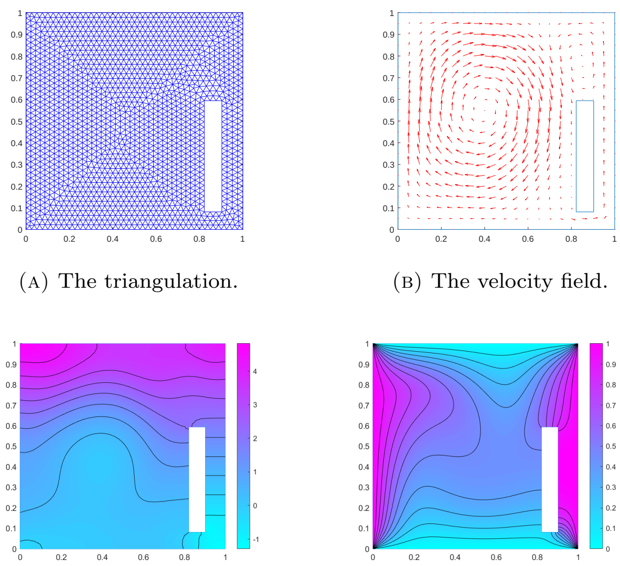

(A) The triangulation. (B) The velocity field.

(C) The isobar. (D) The isotherm.

FIGURE 7. The triangulation and the velocity field, isobar and isotherm of the cavity flow with $Pr = 0.01$, $Ra = 1000$, $k_0 = 0.1$ at mesh size $h = 0.025$.

Acknowledgments

This work is supported by National Natural Science Foundation of China (NO. 11971377).

References

[1] R. A. Adams and J. J. F. Fournier. *Sobolev spaces.* Acdemic Press, Amsterdam, 2003.
[2] A. A. O. Ammi and M. Marion. Nonlinear Galerkin methods and mixed finite elements: two-grid algorithms for the Navier-Stokes equations. *Numer. Math.*, 68(2):189–213, 1994.
[3] I. Babuška and G. N. Gatica. A residual-based a posteriori error estimator for the Stokes-Darcy coupled problem. *SIAM J. Numer. Anal.*, 48(2):498–523, 2010.
[4] F. Bayrak, H. F. Oztop, and F. Selimefendigil. Effects of different fin parameters on temperature and efficiency for cooling of photovoltaic panels under natural convection. *Sol. Energy*, 188:484–494, 2019.
[5] J. Boland and W. Layton. Error analysis for finite element methods for steady natural convection problems. *Numer. Funct. Anal. Optim.*, 11:449–483, 1990.
[6] Y. Boubendir and S. Tlupova. Domain decomposition methods for solving Stokes-Darcy problems with boundary integrals. *SIAM J. Sci. Comput.*, 35(1):B82–B106, 2013.
[7] J. H. Bramble, J. E. Pasciak, and A. H. Schatz. The construction of preconditioners for elliptic problems by substructuring. I. *Math. Comp.*, 47(175):103–134, 1986.
[8] M. Cai, M. Mu, and J. Xu. Numerical solution to a mixed Navier-Stokes/Darcy model by the two-grid approach. *SIAM J. Numer. Anal.*, 47(5):3325–3338, 2009.
[9] X. C. Cai. Additive Schwarz algorithms for parabolic convection-diffusion equations. *Numer. Math.*, 60(1):41–61, 1991.
[10] X. C. Cai. Multiplicative Schwarz methods for parabolic problems. Iterative methods in numerical linear algebra. *SIAM J. Sci. Comput.*, 15(3):587–603, 1994.
[11] Y. Cao, Y. Chu, X.-M. He, and M. Wei. Decoupling the stationary Navier-Stokes-Darcy system with the Beavers-Joseph-Saffman interface condition. *Abstr. Appl. Anal.*, pages Article ID 136483, 10 pages, 2013.
[12] Y. Cao, M. Gunzburger, X.-M. He, and X. Wang. Robin-Robin domain decomposition methods for the steady Stokes-Darcy model with Beaver-Joseph interface condition. *Numer. Math.*, 117(4):601–629, 2011.
[13] Y. Cao, M. Gunzburger, X.-M. He, and X. Wang. Parallel, non-iterative, multi-physics domain decomposition methods for time-dependent Stokes-Darcy systems. *Math. Comp.*, 83(288):1617–1644, 2014.
[14] A. Çibik and S. Kaya. A projection-based stabilized finite element method for steady state natural convection problem. *J. Math. Anal. Appl.*, 381(2):469–484, 2011.
[15] Q. Cheng, X. Yang, and J. Shen. Efficient and accurate numerical schemes for a hydrodynamically coupled phase field diblock copolymer model. *J. Comput. Phys.*, 341:44–60, 2017.
[16] P. Ciarlet. *The finite element method for elliptic problems.* North-Holland, Amsterdam, 1979.
[17] J. M. Connors, J. S. Howell, and W. J. Layton. Partitioned time stepping for a parabolic two domain problem. *SIAM J. Numer. Anal.*, 47(5):3526–3549, 2009.
[18] C. N. Dawson and T. F. Dupont. Explicit/implicit conservative Galerkin domain decomposition procedures for parabolic problems. *Math. Comp.*, 58(197):21–34, 1992.
[19] C. N. Dawson and T. F. Dupont. Explicit/implicit, conservative domain decomposition procedures for parabolic problems based on block-centered finite differences. *SIAM J. Numer. Anal.*, 31(4):1045–1061, 1994.
[20] D. Y. Demezhko, M. G. Mindubaev, and B. D. Khatskevich. Thermal effects of natural convection in boreholes. *Russ. Geol. Geophys.*, 58(10):1270–1276, 2017.
[21] T. Dietrich, C. Röcker, T. Graf, and M. A. Ahmed. Modelling of natural convection in thin-disk lasers. *Appl. Phys. B*, 126(3):1–7, 2020.
[22] M. Discacciati and L. Gerardo-Giorda. Optimized Schwarz methods for the Stokes-Darcy coupling. *IMA J. Numer. Anal.*, 38(4):19591983, 2018.
[23] M. Discacciati, E. Miglio, and A. Quarteroni. Mathematical and numerical models for coupling surface and groundwater flows. *Appl. Numer. Math.*, 43(1-2):57–74, 2002.
[24] M. Discacciati, A. Quarteroni, and A. Valli. Robin-Robin domain decomposition methods for the Stokes-Darcy coupling. *SIAM J. Numer. Anal.*, 45(3):1246–1268, 2007.

[25] M. Dryja and X. Tu. A domain decomposition discretization of parabolic problems. *Numer. Math*, 107(4):625–640, 2007.
[26] Q. Du, M. Mu, and Z. N. Wu. Efficient parallel algorithms for parabolic problems. *SIAM J. Numer. Anal.*, 39(5):1469–1487, 2001/02.
[27] W. Feng, X.-M. He, Z. Wang, and X. Zhang. Non-iterative domain decomposition methods for a non-stationary Stokes-Darcy model with Beavers-Joseph interface condition. *Appl. Math. Comput.*, 219(2):453–463, 2012.
[28] M. Gander. Optimized schwarz methods. *SIAM J. Numer. Anal.*, 44(2):699–731, 2006.
[29] M. J. Gander, F. Magoulès, and F. Nataf. Optimized Schwarz methods without overlap for the Helmholtz equation. *SIAM J. Sci. Comput.*, 24(1):38–60, 2002.
[30] M. J. Gander and H. Zhang. A class of iterative solvers for the Helmholtz equation: factorizations, sweeping preconditioners, source transfer, single layer potentials, polarized traces, and optimized Schwarz methods. *SIAM Rev.*, 61(1):3–76, 2019.
[31] Y. Gao, D. Han, X.-M. He, and U. Rüde. Unconditionally stable numerical methods for Cahn-Hilliard-Navier-Stokes-Darcy system with different densities and viscosities. *J. Comput. Phys.*, 454:#110968, 2022.
[32] Y. Gao, X.-M. He, L. Mei, and X. Yang. Decoupled, linear, and energy stable finite element method for the Cahn-Hilliard-Navier-Stokes-Darcy phase field model. *SIAM J. Sci. Comput.*, 40(1):B110–B137, 2018.
[33] Y. Gao, X.-M. He, and Y. Nie. Second-order, fully decoupled, linearized, and unconditionally stable SAV schemes for Cahn-Hilliard-Darcy system. *Numer. Methods Partial Differential Equations*, page doi: 10.1002/num.22829, 2022.
[34] G. N. Gatica, S. Meddahi, and R. Oyarzúa. A conforming mixed finite-element method for the coupling of fluid flow with porous media flow. *IMA J. Numer. Anal.*, 29(1):86–108, 2009.
[35] V. Girault and P. Raviart. *Finite element methods for Navier-Stokes equations*. Springer-Verlag, Berlin, 1986.
[36] M. Gunzburger, X.-M. He, and B. Li. On Ritz projection and multi-step backward differentiation schemes in decoupling the Stokes-Darcy model. *SIAM J. Numer. Anal.*, 56(1):397–427, 2018.
[37] B. Gvozdić, O. Dung, E. Alméras, D. F. van Gils, D. Lohse, S. G. Huisman, and C. Sun. Experimental investigation of heat transport in inhomogeneous bubbly flow. *Chem. Eng. Sci.*, 198:260–267, 2019.
[38] X.-M. He, N. Jiang, and C. Qiu. An artificial compressibility ensemble algorithm for a stochastic Stokes-Darcy model with random hydraulic conductivity and interface conditions. *Int. J. Numer. Meth. Eng.*, 121(4):712–739, 2020.
[39] X.-M. He, J. Li, Y. Lin, and J. Ming. A domain decomposition method for the steady-state Navier-Stokes-Darcy model with Beavers-Joseph interface condition. *SIAM J. Sci. Comput.*, 37(5):S264–S290, 2015.
[40] J. Hou, D. Hu, X.-M. He, and C. Qiu. Modeling and a Robin-type decoupled finite element method for dual-porosity-Navier-Stokes system with application to flows around multistage fractured horizontal wellbore. *Comput. Meth. Appl. Mech. Eng.*, 388:#114248, 2022.
[41] P. Huang. An efficient two-level finite element algorithm for the natural convection equations. *Appl. Numer. Math.*, 118:75–86, 2017.
[42] P. Huang and W. Li an Z. Si. Several iterative schemes for the stationary natural convection equations at different rayleigh numbers. *Numer. Methods Partial Differential Equations*, 31(3), 2014.
[43] P. Huang, J. Zhao, and X. Feng. An oseen scheme for the conduction-convection equations based on a stabilized nonconforming method. *Appl. Math. Modell.*, 38:535–547, 2014.
[44] P. Huang, J. Zhao, and X. Feng. An oseen scheme for the conduction-convection equations based on a stabilized nonconforming method. *Appl. Math. Modell.*, 38:535–547, 2014.
[45] Q. Huang, X. Yang, and X.-M. He. Numerical approximations for a smectic-A liquid crystal flow model: first-order, linear, decoupled and energy stable schemes. *Discrete Contin. Dyn. Syst. Ser. B*, 23(6):2177–2192, 2018.
[46] T. Jangveladze and Z. Kiguradze. Unique solvability and decomposition method for one nonlinear multi-dimensional integro-differential parabolic equation. *Int. J. Numer. Anal. Mod.*, 17:806–819, 2020.
[47] H. Jiang, X. Zhu, V. Mathai, X. Yang, R. Verzicco, D. Lohse, and C. Sun. Convective heat transfer along ratchet surfaces in vertical natural convection. *J. Fluid Mech.*, 873:1055–1071, 2019.
[48] L. M. Jiji. *Heat Convection*. Springer Berlin Heidelberg, Berlin, Heidelberg, 2006.

[49] H. Kivioja and J. Vinha. Hot-box measurements to investigate the internal convection of highly insulated loose-fill insulation roof structures. *Energy Build.*, 216:109934, 2020.

[50] D. Kumar and B. Premachandran. Effect of atmospheric wind on natural convection based solar air heaters. *Inter. J. Therm. Sci.*, 873:1055–1071, 2019.

[51] W. J. Layton, F. Schieweck, and I. Yotov. Coupling fluid flow with porous media flow. *SIAM J. Numer. Anal.*, 40(6):2195–2218, 2002.

[52] F. Lin, X.-M. He, and X. Wen. Fast, unconditionally energy stable large time stepping method for a new Allen-Cahn type square phase-field crystal model. *Appl. Math. Lett.*, 92:248–255, 2019.

[53] P.-L. Lions. On the Schwarz alternating method. I. In *First International Symposium on Domain Decomposition Methods for Partial Differential Equations (Paris, 1987)*, pages 1–42. SIAM, Philadelphia, PA, 1988.

[54] P.-L. Lions. On the Schwarz alternating method. III. a variant for nonoverlapping subdomains. In *Third International Symposium on Domain Decomposition Methods for Partial Differential Equations (Houston, TX, 1989)*, pages 202–223. SIAM, Philadelphia, PA, 1990.

[55] Y. Liu, Y. He, X. Li, and X.-M. He. A novel convergence analysis of Robin-Robin domain decomposition method for Stokes-Darcy system with Beavers-Joseph interface condition. *Appl. Math. Lett.*, 119:#107181, 2021.

[56] C. Lu, J. Wan, Y. Cao, and X.-M. He. A fully decoupled iterative method with three-dimensional anisotropic immersed finite elements for Kaufman-type discharge problems. *Comput. Meth. Appl. Mech. Eng.*, 372:#113345, 2020.

[57] Z. D. Luo and X. M. Lu. A least-squares galerkin/petrov mixed finite element method for stationary conduction-convection problems. *Math. Numer. Sin.*, 25:231–244, 2003.

[58] Md. A. Al Mahbub, X.-M. He, N. J. Nasu, C. Qiu, Y. Wang, and H. Zheng. A coupled multi-physics model and a decoupled stabilized finite element method for closed-loop geothermal system. *SIAM J. Sci. Comput.*, 42(4):B951–B982, 2020.

[59] Md. A. Al Mahbub, X.-M. He, N. J. Nasu, C. Qiu, and H. Zheng. Coupled and decoupled stabilized mixed finite element methods for non-stationary dual-porosity-Stokes fluid flow model. *Int. J. Numer. Meth. Eng.*, 120(6):803–833, 2019.

[60] M. Marion and J. Xu. Error estimates on a new nonlinear galerkin method based on two-grid finite elements. *SIAM J. Numer. Anal.*, 32(4):1170–1184, 1995.

[61] M. Mu and J. Xu. A two-grid method of a mixed Stokes-Darcy model for coupling fluid flow with porous media flow. *SIAM J. Numer. Anal.*, 45(5):1801–1813, 2007.

[62] M. Mu and X. Zhu. Decoupled schemes for a non-stationary mixed Stokes-Darcy model. *Math. Comp.*, 79(270):707–731, 2010.

[63] J. P. Panda, K. Sasmal, and H. V. Warrior. A non-linear eddy viscosity model for turbulent natural convection in geophysical flows. *Inter. J. Environ. Ecol. Eng.*, 12(3):182–189, 2018.

[64] Z. Qiao, S. Sun, T. Zhang, and Y. Zhang. A new multi-component diffuse interface model with Peng-Robinson equation of state and its scalar auxiliary variable (SAV) approach. *Commun. Comput. Phys.*, 26(5):1597–1616, 2019.

[65] C. Qiu, X.-M. He, J. Li, and Y. Lin. A domain decomposition method for the time-dependent Navier-Stokes-Darcy model with Beavers-Joseph interface condition and defective boundary condition. *J. Comput. Phys.*, 411:#109400, 2020.

[66] A. Quarteroni and A. Valli. *Domain decomposition methods for partial differential equations*. Numerical Mathematics and Scientific Computation. Oxford Science Publications, New York, 1999.

[67] M. Sarai and D. Liang. Even-odd cycled high-order splitting finite difference time domain method for Maxwell's equations. *Int. J. Numer. Anal. Mod.*, 18:79–99, 2021.

[68] L. Shan and H. Zheng. Partitioned time stepping method for fully evolutionary Stokes-Darcy flow with Beavers-Joseph interface conditions. *SIAM J. Numer. Anal.*, 51(2):813–839, 2013.

[69] J. Shen, J. Xu, and J. Yang. The scalar auxiliary variable (SAV) approach for gradient flows. *J. Comput. Phys.*, 353:407–416, 2018.

[70] J. Shen, J. Xu, and J. Yang. A new class of efficient and robust energy stable schemes for gradient flows. *SIAM Rev.*, 61(3):474–506, 2019.

[71] J. Shen and X. Yang. Decoupled, energy stable schemes for phase-field models of two-phase incompressible flows. *SIAM J. Numer. Anal.*, 53(1):279–296, 2015.

[72] D. Shi and J. Ren. Nonconforming mixed finite element method for the stationary conduction-convection problem. *Int. J. Numer. Anal. Model.*, 6(2):293–31, 2009.

[73] H. Shi and H. Liao. Unconditional stability of corrected explicit-implicit domain decomposition algorithms for parallel approximation of heat equations. *SIAM J. Numer. Anal.*, 44(4):1584–1611, 2006.

[74] Z. Si, Y. Shang, and T. Zhang. New one-and two-level newton iterative mixed finite element methods for stationary conductionconvection problems. *Finite Elem. Anal. Des.*, 47(2):175–183, 2011.

[75] T. Sohail, B. Gayen, and A. McC. Hogg. The dynamics of mixed layer deepening during open-ocean convection. *J. Phys. Oceanogr.*, 50(6):1625–1641, 2020.

[76] C. Taylor and P. Hood. A numerical solution of the navier-stokes equations using the finite element technique. *Comput. Fluids*, 1(1):73–100, 1973.

[77] R. Temam. *Navier-Stokes equations theory and numerical analysis*. North-Holland, Amsterdam, 1979.

[78] E. Toghroli and S. A. R. Gandjalikhan Nassab. Numerical analysis of inclined double pane windows with considering combined natural convection and radiation in filling gas. *Modares Mech. Eng.*, 19(9):2235–2245, 2019.

[79] A. Toselli and O. Widlund. *Domain decomposition methods-algorithms and theory*, volume 34 of *Springer Series in Computational Mathematics*. Springer-Verlag, Berlin, 2005.

[80] E. A. Villagrán, E. J. B. Romero, and C. R. Bojacá. Transient cfd analysis of the natural ventilation of three types of greenhouses used for agricultural production in a tropical mountain climate. *Biosyst. Eng.*, 188:288–304, 2019.

[81] C. Xu, C. Chen, X. Yang, and X.-M. He. Numerical approximations for the hydrodynamics coupled binary surfactant phase field model: second order, linear, unconditionally energy stable schemes. *Commun. Math. Sci.*, 17(3):835–858, 2019.

[82] J. Xu. A novel two-grid method for semilinear elliptic equations. *SIAM J. Sci. Comput.*, 15(1):231–237, 1994.

[83] J. Xu. Two-grid discretization techniques for linear and nonlinear PDEs. *SIAM J. Numer. Anal.*, 33(5):1759–1777, 1996.

[84] J. Xu and J. Zou. Some nonoverlapping domain decomposition methods. *SIAM Rev.*, 40(4):857–914, 1998.

[85] X. Yang. A novel fully-decoupled, second-order and energy stable numerical scheme of the conserved Allen-Cahn type flow-coupled binary surfactant model. *Comput. Meth. Appl. Mech. Eng.*, 373:#113502, 2021.

[86] X. Yang. Efficient and Energy Stable scheme for the hydrodynamically coupled three components Cahn-Hilliard phase-field model using the stabilized-Invariant Energy Quadratization (S-IEQ) Approach. *J. Comput. Phys.*, 438:110342, 2021.

[87] X. Yang. On a novel fully decoupled, second-order accurate energy stable numerical scheme for a binary fluid-surfactant phase-field model. *SIAM J. Sci. Comput.*, 43(2):B479–B507, 2021.

[88] X. Yang and D. Han. Linearly first- and second-order, unconditionally energy stable schemes for the phase field crystal equation. *J. Comput. Phys.*, 330:1116–1134, 2017.

[89] X. Yang and X.-M. He. A fully-discrete decoupled finite element method for the conserved AllenCahn type phase-field model of three-phase fluid flow system. *Comput. Meth. Appl. Mech. Eng.*, 389:#114376, 2022.

[90] X. Yang and L. Ju. Linear and unconditionally energy stable schemes for the binary fluid-surfactant phase field model. *Comput. Methods Appl. Mech. Engrg.*, 318:1005–1029, 2017.

[91] X. Yang, J. Zhao, and X.-M. He. Linear, second order and unconditionally energy stable schemes for the viscous Cahn-Hilliard equation with hyperbolic relaxation using the invariant energy quadratization method. *J. Comput. Appl. Math.*, 343(1):80–97, 2018.

[92] X. Yang, J. Zhao, and Q. Wang. Numerical approximations for the molecular beam epitaxial growth model based on the invariant energy quadratization method. *J. Comput. Phys.*, 333:104–127, 2017.

[93] Y. B. Yang and Y. L. Jiang. Numerical analysis and computation of a type of imex method for the time-dependent natural convection problem. *Comput. Methods Appl. Math.*, 16(2):321–344, 2016.

[94] G. Zhang, X.-M. He, and X. Yang. A decoupled, linear and unconditionally energy stable scheme with finite element discretizations for magneto-hydrodynamic equations. *J. Sci. Comput.*, 81:1678–1711, 2019.

[95] G. Zhang, X.-M. He, and X. Yang. Decoupled, linear, and unconditionally energy stable fully-discrete finite element numerical scheme for a two-phase ferrohydrodynamics model. *SIAM J. Sci. Comput.*, 43(1):B167–B193, 2021.

[96] G. Zhang, X.-M. He, and X. Yang. A fully decoupled linearized finite element method with second-order temporal accuracy and unconditional energy stability for incompressible MHD equations. *J. Comput. Phys.*, 448:#110752, 2022.
[97] H. Zhang, X. Yang, and J. Zhang. Stabilized invariant energy quadratization (S-IEQ) method for the molecular beam epitaxial model without slope section. *Int. J. Numer. Anal. Model.*, 18:642–655, 2021.
[98] J. Zhang and X. Yang. Numerical approximations for a new L2-gradient flow based phase field crystal model with precise nonlocal mass conservation. *Comput. Phys. Commun.*, 243:51–67, 2019.
[99] J. Zhang and X. Yang. On Efficient numerical schemes for a two-mode phase field crystal model with face-centered-cubic (FCC) ordering structure. *Appl. Numer. Math.*, 146:13–37, 2019.
[100] J. Zhang and X. Yang. Efficient and accurate numerical scheme for a magnetic-coupled phase-field-crystal model for ferromagnetic solid materials. *Comput. Methods Appl. Mech. Eng.*, 371:113110, 2020.
[101] Y. Zhang, Y. Hou, and H. Zuo. A posteriori error estimation and adaptive computation of conduction convection problems. *Appl. Math. Modell.*, 35:2336–2347, 2011.
[102] J. Zhao, X. Yang, J. Shen, and Q. Wang. A decoupled energy stable scheme for a hydrodynamic phase-field model of mixtures of nematic liquid crystals and viscous fluids. *J. Comput. Phys.*, 305:539–556, 2016.
[103] Z. Zheng, B. Simeon, and L. Petzold. A stabilized explicit lagrange multiplier based domain decomposition method for parabolic problems. *J. Comput. Phys.*, 227(10):5272–5285, 2008.
[104] L. Zhu, G. Yuan, and Q. Du. An efficient explicit/implicit domain decomposition method for convection-diffusion equations. *Numer. Methods Partial Differential Equations*, 26(4):852–873, 2010.
[105] Y. Zhuang and X. H. Sun. Stabilized explicit-implicit domain decomposition methods for the numerical solution of parabolic equations. *SIAM J. Sci. Comput.*, 24(1):335–358, 2002.

School of Mathematics and Statistics, Xi'an Jiaotong University, Xi'an 710049, PRC
E-mail: hyy_alpha@163.com

School of Mathematics and Statistics, Xi'an Jiaotong University, Xi'an 710049, PRC
E-mail: wenjingyan@mail.xjtu.edu.cn

Department of Mathematics and Statistics, Missouri University of Science and Technology, Rolla 65409, USA
E-mail: lbc4r@mst.edu

Department of Mathematics and Statistics, Missouri University of Science and Technology, Rolla 65409, USA
E-mail: hex@mst.edu